Appendix D
Effects of Spectrum Matching on Characteristics of Earthquake Ground Motion Time-Histories

D.1 Introduction

a. This appendix describes evaluations of the effects of spectrum matching on the characteristics of earthquake ground motion time-histories. The approach used in this examination was to select recorded natural earthquake strong motion time-histories; these selected time-histories were then scaled to provide a visual average fit and spectrally modified to provide a close fit to a target response spectrum. The effects of spectral matching were assessed by comparing the basic characteristics of the scaled time-histories with those of the spectrally matched time-histories.

b. The spectrum matching technique used in this study is based on the method originally developed by Lilhanand and Tseng (1988) for time-domain modifications of a time-history so that its response spectrum closely matches a prescribed smooth response spectrum. The technique is described in Appendix C.

D.2 Selection of Earthquake Ground Motion Time-Histories

a. The postulated design earthquake for these evaluations was a moment magnitude M_W 6.5 reverse faulting event located 5 km from the site of interest. For this design earthquake, a smooth design response spectrum (5 percent damping) of site ground motions was constructed for the period range of 0 to 0.6 sec. This period range was selected for spectrum matching in these evaluations because it encompasses the fundamental periods of most concrete hydraulic structures.

b. Ten earthquake strong ground motion time-histories were selected for matching to the smooth response spectrum. In selecting these time-histories, earthquake magnitude, source-to-site distance, and ground motion characteristics (amplitude and frequency content) were considered. Table D-1 lists the selected time-histories and their associated magnitudes and distances. The time-histories were recorded at sites underlain by rock, except for one record that was recorded on a stiff soil site, during earthquakes having moment magnitudes in the range of 6.2 to 7.0 at closest earthquake-source-to-site distances less than 12 km except for one record obtained at 17 km. To reduce the changes that occur to the characteristics of the original time-histories as a result of spectrum matching, time-histories were selected that have response spectral shapes that were generally somewhat similar to the smooth design site response spectrum in the period range of 0 to 0.6 sec.

D.3 Scaling and Spectrum Matching of Time-Histories

a. Each time-history was scaled to the approximate level of the design response spectrum. The scaling factors were obtained by visually "fitting" each response spectrum to the smooth response spectrum, such that spectral peaks would tend to exceed the smooth spectrum, and spectral valleys would tend to lie below it. The scaling factors for the selected time-histories are given in Table D-1. Baseline-corrected time-histories of acceleration, velocity, and displacement of these scaled records are shown in Figures D-1 through D-10. The response spectra of all the scaled time-histories are plotted in Figure D-11, along with the smooth response spectrum. The spectra of the individual scaled time-histories are plotted in Figures D-12 through D-21.

Table D-1
List of Selected Time-Histories

Earthquake	Year	Station	Site	Comp.	M_W	R, km	Scale Factor
San Fernando, CA	1971	279	Rock	254	6.6	2.8	0.60
Gazli, USSR	1976	9201	Rock	90	6.8	3.0	0.75
Morgan Hill, CA	1984	57217	Rock	195	6.2	0.1	0.86
Loma Prieta, CA	1989	UCSCB	Rock	90	7.0	10.3	1.00
		47006	Rock	67	7.0	11.6	1.50
Cape Mendocino, CA	1992	89005	Rock	0	7.0	8.5	0.44
Northridge, CA	1994	6273	Rock	18	6.7	7.8	0.83
		24207	Rock	265	6.7	9.8	1.68
		24436	Rock	90	6.7	16.8	0.33
		24279	Soil	90	6.7	7.6	0.89

Note: M_W = moment magnitude.
R = closest distance from recording station to ruptured fault.

b. After the time-histories were scaled, each time-history was then "matched" to the smooth target spectrum using the method of Lilhanand and Tseng (1988). Note that the spectral characteristics of the time-histories were modified only for periods less than 0.6 sec; at longer periods, the spectral characteristics of the original scaled time-histories were only slightly changed by specifying that the spectra of the original scaled time-histories were also the target spectra and baseline-correcting the spectrum-matched time-histories.

c. Figures D-12 to D-21 show the spectra of the individual scaled time-histories before and after spectrum matching, as well as the target spectrum. Figures D-22 through D-31 show the baseline-corrected time-histories for acceleration, velocity, and displacement for the spectrally matched time-histories.

d. Visual examination of the scaled time-histories (Figures D-1 through D-10) and spectrally matched time-histories (Figures D-22 through D-31) indicates that, in general, the spectrum matching process did not greatly change the time-domain character of the ground motions. The time series of accelerations and velocities are generally similar for the scaled and spectrally matched time-histories, especially for time-histories having scaled spectra that are more similar in shape to the target smooth spectrum. Examination of Figures D-12 through D-21 shows that the matching process achieved a close match to the target smooth spectrum except that a good match was sometimes not possible for very high frequency motions (frequencies equal to or greater than about 25 Hz (periods equal to or less than 0.04 sec).

D.4 Analysis of Characteristics of Time-Histories

a. To quantify the effects of spectrum matching, several characteristics of the scaled time-histories before and after spectrum matching were compared. These characteristics include peak ground acceleration (PGA), effective peak acceleration A_E, root-mean-square acceleration (RMS), peak ground velocity (PGV), peak ground displacement (PGD), strong motion duration T_D, energy E, rate of energy input (power) R, and absolute input energy (IE) to an elastic single-degree-of-freedom oscillator.

b. The definitions of effective peak acceleration, root-mean-square acceleration, strong motion duration, energy, and rate of energy input (power) follow those of Kennedy et al. (1984) and are given below.

(1) Strong motion duration T_D:

$$T_D = T_{0.75} - T_{0.05} \tag{D-1}$$

where $T_{0.75}$ and $T_{0.05}$ represent the times at which 75 percent and 5 percent, respectively, of the total energy (defined in (2) below) have been reached. This definition of strong motion duration is slightly different from that of Kennedy et al. (1984), in which the strong motion duration is defined by the larger of $T_{0.75}$ and the time associated with the first zero crossing following the peak acceleration. This definition of strong motion duration was proposed for stiff structures as an alternative to a more common definition of strong duration, which is:

$$T_D = T_{0.95} - T_{0.05} \tag{D-2}$$

where $T_{0.95}$ is the time associated with 95 percent of the total energy. The definition proposed by Kennedy et al. (1984) thus represents a shorter estimate for the strong motion duration; the shorter duration is based on observations that many ground motion records contain long tails of oscillation having significantly lower amplitudes.

(2) Energy E:

$$E = \int_{0}^{T_D} a^2(t)\,dt \tag{D-3}$$

where $a(t)$ is the ground motion acceleration as function of time t. In this analysis, E is calculated over the strong motion duration, $T_D = T_{0.75} - T_{0.05}$. Equation D-3 was proposed by Arias (1970) as a measure of the energy of a ground motion record.

(3) Rate of energy input or power R:

$$R = \frac{E}{T_D} \tag{D-4}$$

where T_D is taken equal to $T_{0.75} - T_{0.05}$.

(4) Root-mean-square acceleration RMS and effective acceleration A_E:

$$RMS = \sqrt{R} \tag{D-5}$$

The RMS acceleration is a statistical average of the absolute values of ground motion accelerations, taken over the strong motion duration T_D. The RMS acceleration can be used as a basis for selecting a design value of acceleration (effective acceleration). Assuming that ground motion can be modeled by a stationary random Gaussian motion, Vanmarcke and Lai (1980) have shown that the effective acceleration of a ground motion record can be expressed as:

$$A_E = K_P * RMS \tag{D-6}$$

$$K_P = \sqrt{2\ ln\ (2.8T_D / T_0)} \tag{D-7}$$

where T_0 is the predominant period of ground motion.

(5) Absolute input energy IE to an elastic single-degree-of-freedom oscillator is defined as (Mahin and Lin 1983):

$$IE = \int -[C\dot{u}(t) + Ku(t)]\dot{u}_g \, dt \tag{D-8}$$

where

C and K = damping and stiffness coefficients, respectively, for an elastic system

$u(t)$ = displacement of the system relative to the ground

$u_g(t)$ = displacement of the ground relative to a fixed reference axis

Input energy was calculated using the computer program NONSPEC (Mahin and Lin 1983). For this study, the input energy averaged over the period range of 0 to 0.6 sec was used. Part of the input energy is absorbed by the system (structure), and the rest is dissipated through viscous damping and inelastic (hysteretic) deformations.

c. Tables D-2 and D-3 summarize these characteristics for the scaled and spectrally matched time-histories, respectively. The ratios of ground motion characteristics between the spectrally matched and scaled time-histories are tabulated in Table D-4. The characteristics of the scaled and spectrally matched time-histories are compared in Figures D-32 through D-41.

d. The degree of alteration of the ground motion characteristics as a result of spectrum matching depends on sensitivity of a characteristic with respect to the changes in the amplitude and frequency content of the ground motions; numerical algorithm of the spectrum matching technique; and degree of initial spectral mismatch (before matching) of the scaled time-history and the target spectrum.

Table D-2
Summary of the Characteristics of the Scaled Time-Histories

Earthquake	Station	Comp	T_D^1 sec	T_D^2 sec	E g·g·sec	R g·g	PGA g	RMS g	A_E g	PGV cm/sec	PGD cm	IE (0-0.6 sec) cm/sec
San Fernando	279	254	5.84	7.22	0.13813	0.02364	0.65	0.15	0.46	33.9	7.09	45.78
Gazli	9201	90	5.37	6.74	0.12958	0.02412	0.52	0.16	0.49	35.4	7.3	38.24
Morgan Hill	57217	195	2.30	3.52	0.10018	0.04354	0.56	0.21	0.54	44.7	9.20	31.43
Loma Prieta	UCSCB	90	6.96	9.86	0.24087	0.03458	0.50	0.19	0.57	44.6	6.4	75.90
	47006	67	1.56	4.98	0.09248	0.05929	0.53	0.24	0.62	43.8	8.7	33.83
Cape Mendocino	89005	0	2.94	13.78	0.05122	0.01742	0.66	0.13	0.37	56.3	22.3	20.69
Northridge	6273	18	3.78	7.21	0.14157	0.03745	0.69	0.19	0.52	97.2	32.6	--
	24436	90	6.52	10.70	0.11238	0.01724	0.59	0.13	0.40	51.60	7.7	40.85
	24207	265	2.02	4.10	0.09230	0.04569	0.73	0.21	0.55	36.2	10.3	46.37
	24279	90	2.82	5.92	0.15517	0.05503	0.52	0.23	0.60	66.5	15.8	66.67
Average	--	--	4.01	7.41	0.12530	0.03580	0.59	0.18	0.51	51.0	12.7	44.42

Note: Parameters are defined in text.
T_D^1: Strong duration between 5 and 75 percent of total energy.
T_D^2: Strong duration between 5 and 95 percent of total energy.

Table D-3
Summary of the Characteristics of the Spectrally Matched Time-Histories

Earthquake	Station	Comp	T_D^1 sec	T_D^2 sec	E g·g·sec	R g·g	PGA g	RMS g	A_E g	PGV cm/sec	PGD cm	IE (0-0.6 sec) cm/sec
San Fernando	279	254	5.44	7.02	0.14963	0.02751	0.59	0.17	0.49	32.8	8.3	53.78
Gazli	9201	90	5.13	6.73	0.15741	0.03067	0.58	0.18	0.54	34.7	6.9	52.03
Morgan Hill	57217	195	3.08	4.48	0.10283	0.03339	0.64	0.18	0.50	41.2	9.5	35.96
Loma Prieta	UCSCB	90	7.90	11.27	0.23827	0.03016	0.51	0.17	0.54	43.1	4.9	69.10
	47006	67	2.66	5.52	0.11499	0.04323	0.50	0.21	0.58	31.8	8.4	35.71
Cape Mendocino	89005	0	1.34	4.48	0.05889	0.04395	0.74	0.21	0.49	59.0	22.0	33.92
Northridge	6273	18	3.68	6.55	0.13219	0.03587	0.74	0.19	0.51	101.0	29.8	--
	24436	90	6.16	9.94	0.14255	0.02314	0.63	0.15	0.46	34.4	8.5	49.54
	24207	265	3.08	5.90	0.13988	0.04542	0.60	0.21	0.60	43.2	8.1	45.50
	24279	90	4.48	10.66	0.17222	0.03844	0.61	0.20	0.55	52.9	17.5	58.15
Average	--	--	4.29	7.25	0.14100	0.03510	0.61	0.19	0.53	47.4	12.4	48.19

Note: Parameters are defined in text.
T_D^1: Strong duration between 5 and 75 percent of total energy.
T_D^2: Strong duration between 5 and 95 percent of total energy.

e. The results of the analyses for this examination generally indicate that the spectrum matching technique did not alter the ground motion characteristics greatly. Spectrum matching, however, increased on average the energy, power, and strong motion duration of the ground motions. From the analyzed time-histories, an average increase of about 10 to 20 percent in the strong motion duration, power, and energy content of a ground motion occurred as a result of spectrum matching (Table D-4).

f. For the 1992 Cape Mendocino record, spectrum matching produces much shorter strong motion duration. With only about 16 percent increase in the total energy of this record, the shorter duration results in much higher calculated power for the spectrally matched time-history (about 2.6 times higher). Spectrum matching also results in higher effective and RMS accelerations for the 1992 Cape Mendocino record. As shown in Figure D-6, the Cape Mendocino time-history is unusual in that it contains a single peak that is three times higher than any other peak of the accelerogram. The spectral shape of this record is much different from the smooth spectrum over the period range of matching (0 to 0.6 sec), being substantially lower in the period range 0.3 to 0.6 sec and substantially higher at periods less than 0.2 sec (Figure D-17).

g. Figures D-42 through D-51 present the correlations of initial spectral mismatch and the degree of alteration for the analyzed ground motion characteristics. Initial spectral mismatch $*(T)$ at a period T is defined as follows:

$$\delta(T) = \frac{\left| Sa(T) - Sa(T)_{Target} \right|}{Sa(T)_{Target}} \tag{D-9}$$

where $Sa(T)$ and $Sa(T)_{Target}$ are the response spectral ordinates of the scaled time-history (before matching) and the target spectrum, respectively, at the period T. Two measures of initial mismatch, over the period range of 0 to 0.6 sec, were used for this study:

Table D-4
Ratios of the Characteristics Between Spectrally Matched and Scaled Time-Histories

Earthquake	Station	Comp	T_D^1 sec	T_D^2 sec	E g·g·sec	R g·g	PGA g	RMS g	A_E g	PGV cm/sec	PGD cm	IE (0-0.6 sec) cm/sec
San Fernando	279	254	0.931	0.972	1.087	1.167	0.908	1.133	1.065	0.968	1.171	1.175
Gazli	9201	90	0.956	0.998	1.215	1.292	1.115	1.125	1.102	0.980	0.945	1.361
Morgan Hill	57217	195	1.339	1.273	1.030	0.750	1.143	0.857	0.926	0.922	1.033	1.144
Loma Prieta	UCSCB	90	1.134	1.142	0.988	0.857	1.020	0.895	0.947	0.996	0.766	0.910
	47006	67	1.705	1.108	1.250	0.729	0.943	0.875	0.935	0.726	0.966	1.056
Cape Mendocino	89005	0	0.456	0.325	1.157	2.588	1.121	1.165	1.324	1.048	0.987	1.639
Northridge	6273	18	0.975	0.908	0.930	0.973	1.072	1.000	0.981	1.039	0.914	--
	24436	90	0.945	0.927	1.277	1.353	1.068	1.154	1.150	0.667	1.104	1.213
	24207	265	1.525	1.439	1.522	0.978	0.822	1.000	1.091	1.193	0.786	0.981
	24279	90	1.589	1.800	1.110	0.691	1.173	0.870	0.917	0.795	1.108	0.872
Average	--	--	1.155	1.09	1.156	1.138	1.039	1.052	1.044	0.930	0.978	1.150

Note: Parameters are defined in text.
T_D^1: Strong duration between 5 and 75 percent of total energy.
T_D^2: Strong duration between 5 and 95 percent of total energy.

(1) Average mismatch $*_{ave}$:

$$\delta_{ave} = Average\ \{\delta(T_1),.....,\delta(T_N)\}\} \tag{D-10}$$

(2) Maximum mismatch $*_{max}$:

$$\delta_{max} = Maximum\{\delta(T_1),.....,\delta(T_N)\}\} \tag{D-11}$$

where T_1 and T_N are the N discrete periods over the period range of 0 to 0.6 sec.

h. Figures D-42 through D-51 show that there are no apparent correlations between the analyzed ground motion characteristics and average or maximum mismatch, with the exception that a positive correlation may be inferred for the peak ground acceleration (Figure D-42).

i. It should be noted that this study is based on a relatively limited number of records. These records were selected because their initial spectral shapes are generally similar to that of the target smooth design spectrum. The lack of correlation between the analyzed characteristics and initial spectral mismatch may be due to the fact that overall initial mismatch is relatively small.

j. Figure D-51 and Table D-4 indicate that, except for the Gazli and Cape Mendocino records, the input energy of the spectrally matched and scaled records are within a factor of about 1.2 of each other. The larger differences for the Gazli and Cape Mendocino records are likely due to the poor match at periods greater than 0.2 to 0.3 sec between the spectra of the scaled time-histories and the smooth spectrum, as shown in Figures D-13 and D-17.

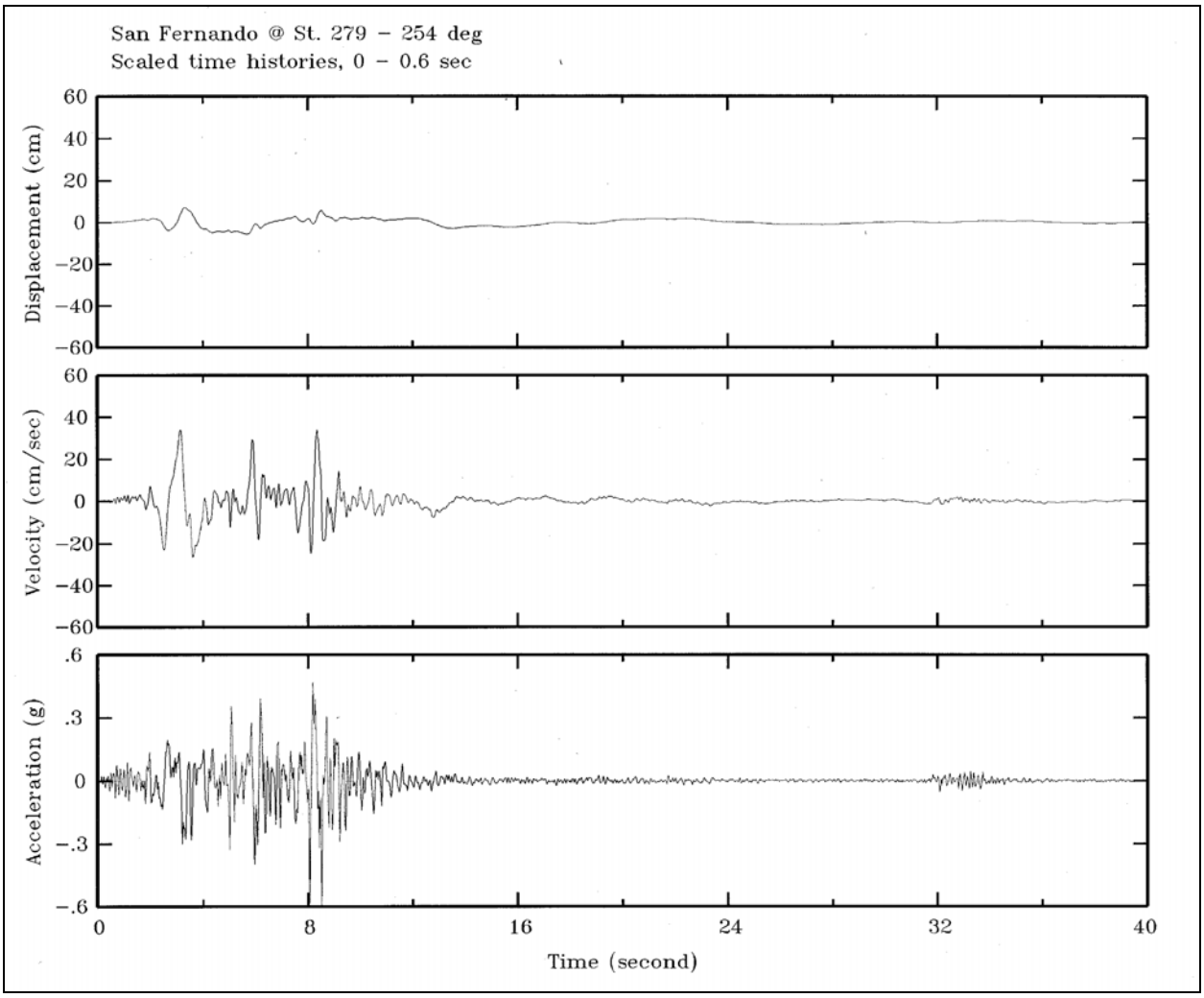

Figure D-1. Scaled time-histories of acceleration, velocity, and displacement for the 1971 San Fernando earthquake recorded at station 279

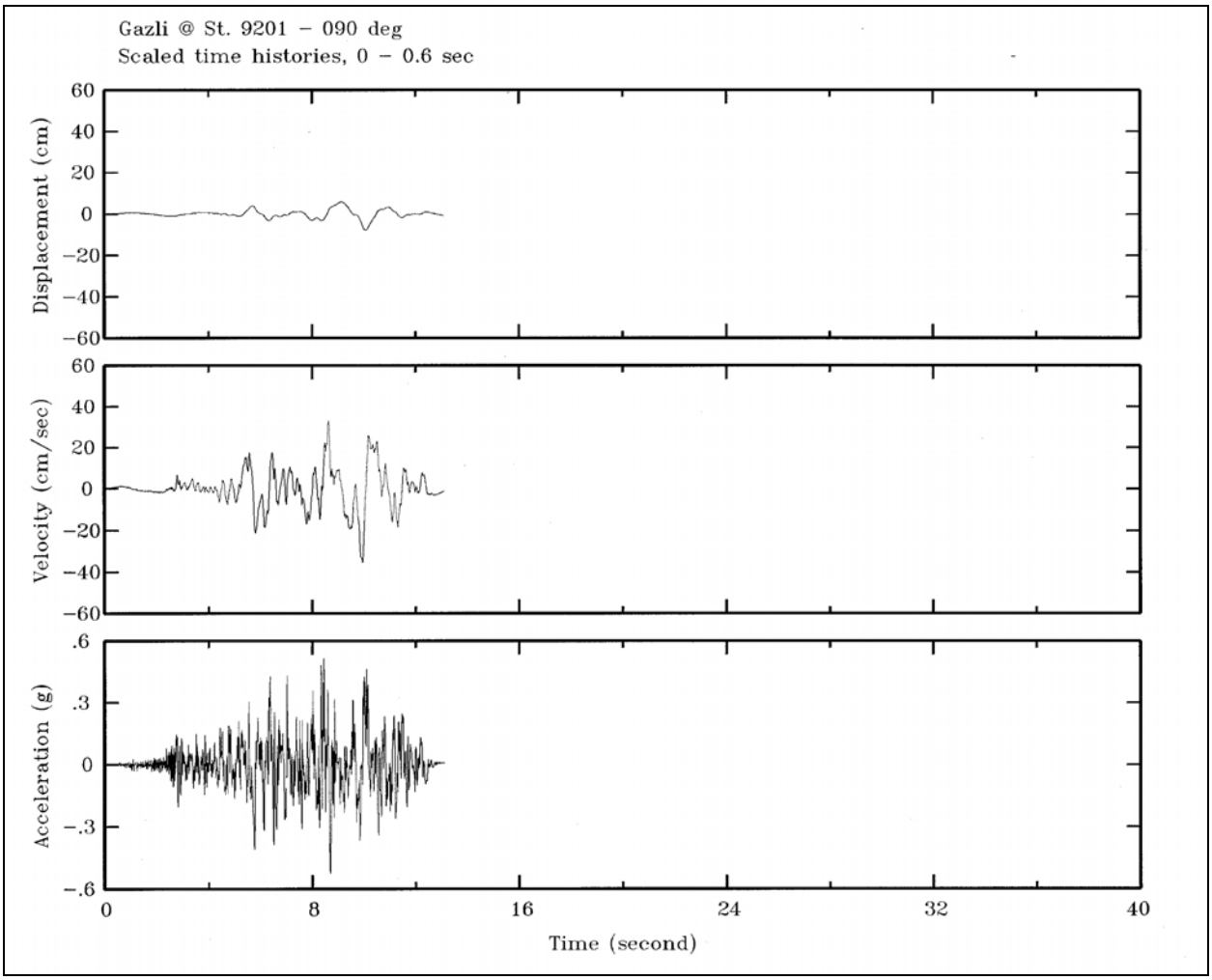

Figure D-2. Scaled time-histories of acceleration, velocity, and displacement for the 1976 Gazli earthquake recorded at Gazli

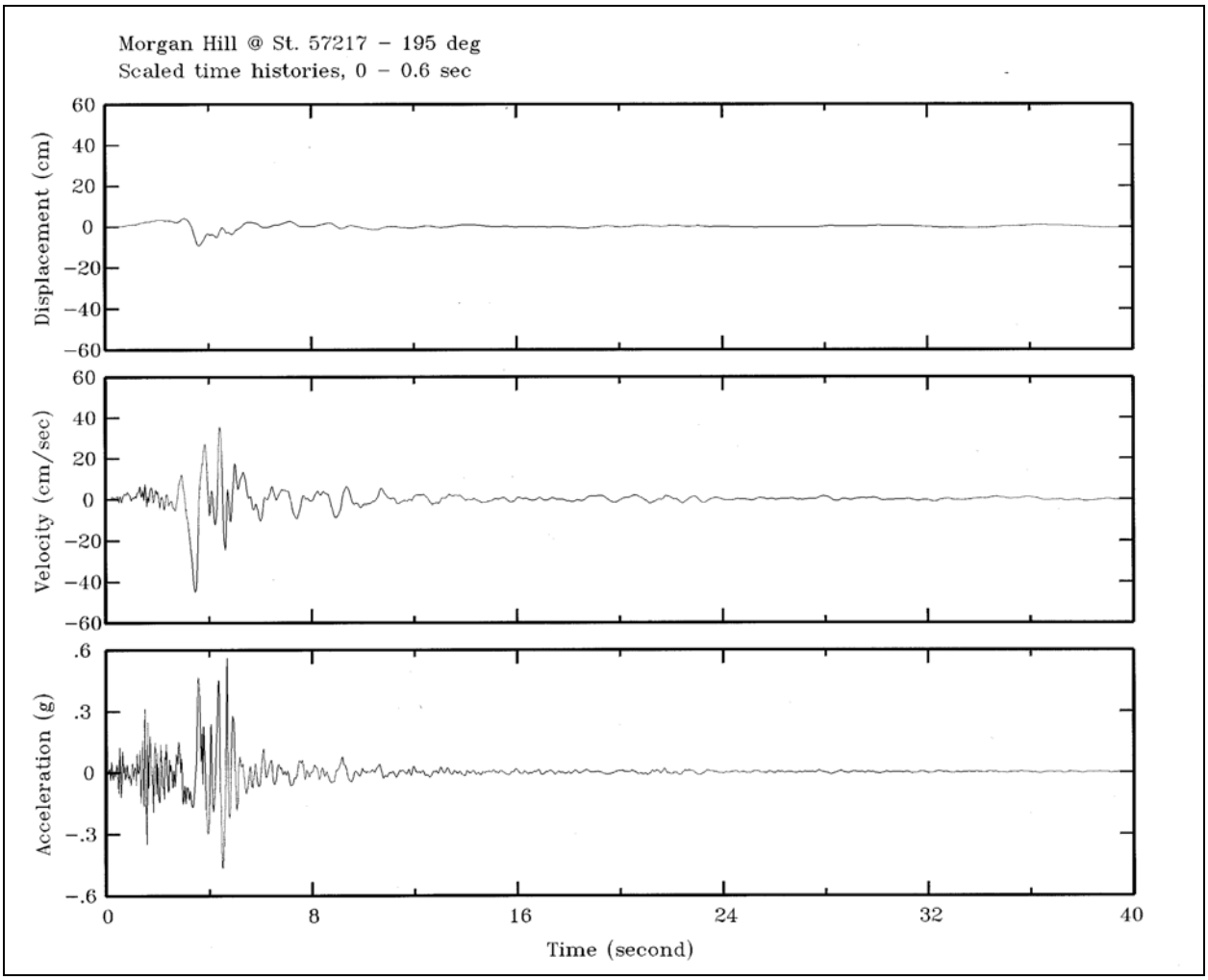

Figure D-3. Scaled time-histories of acceleration, velocity, and displacement for the 1984 Morgan Hill earthquake recorded at station 57217

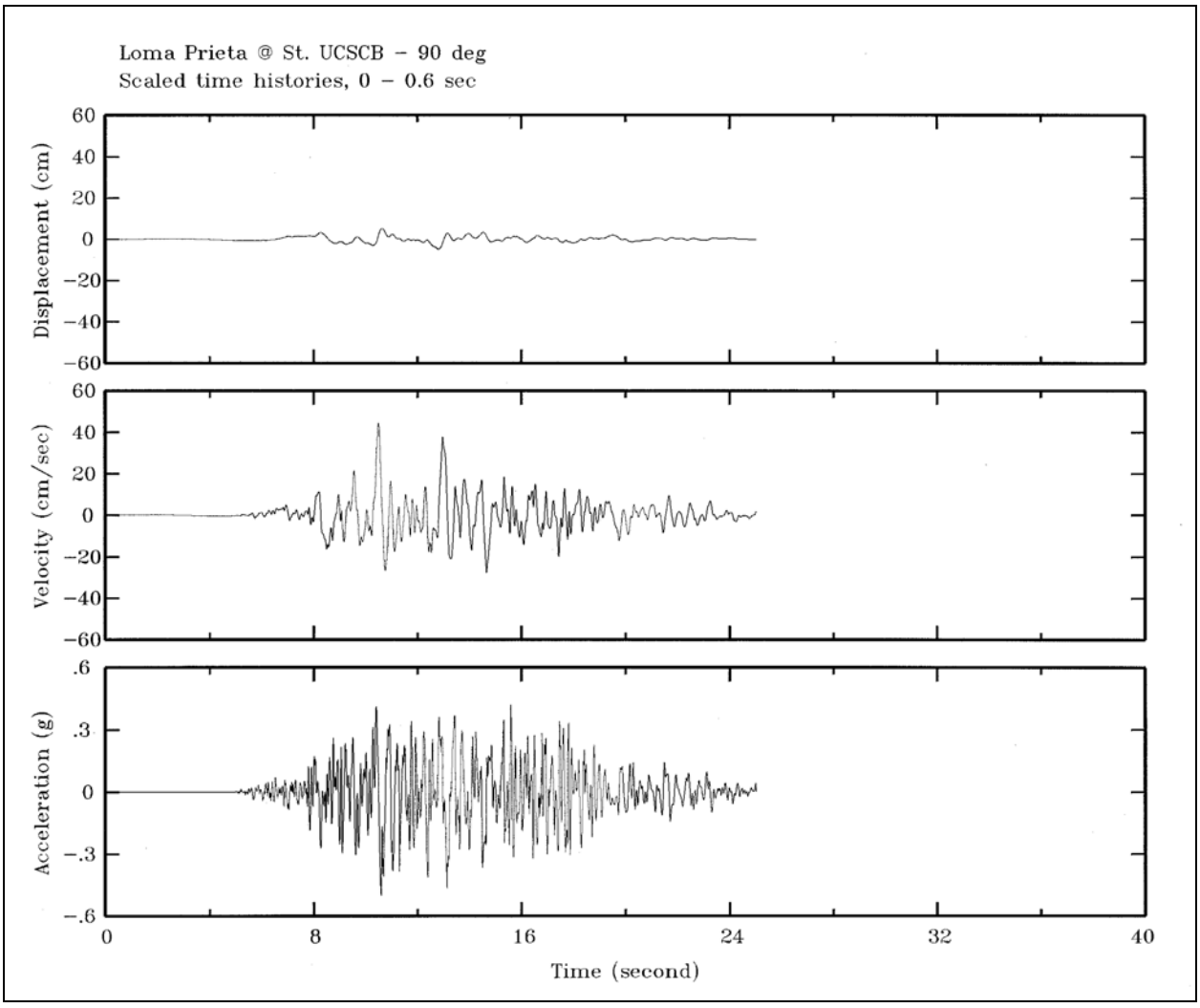

Figure D-4. Scaled time-histories of acceleration, velocity, and displacement for the 1989 Loma Prieta earthquake recorded at UCSC Brane building

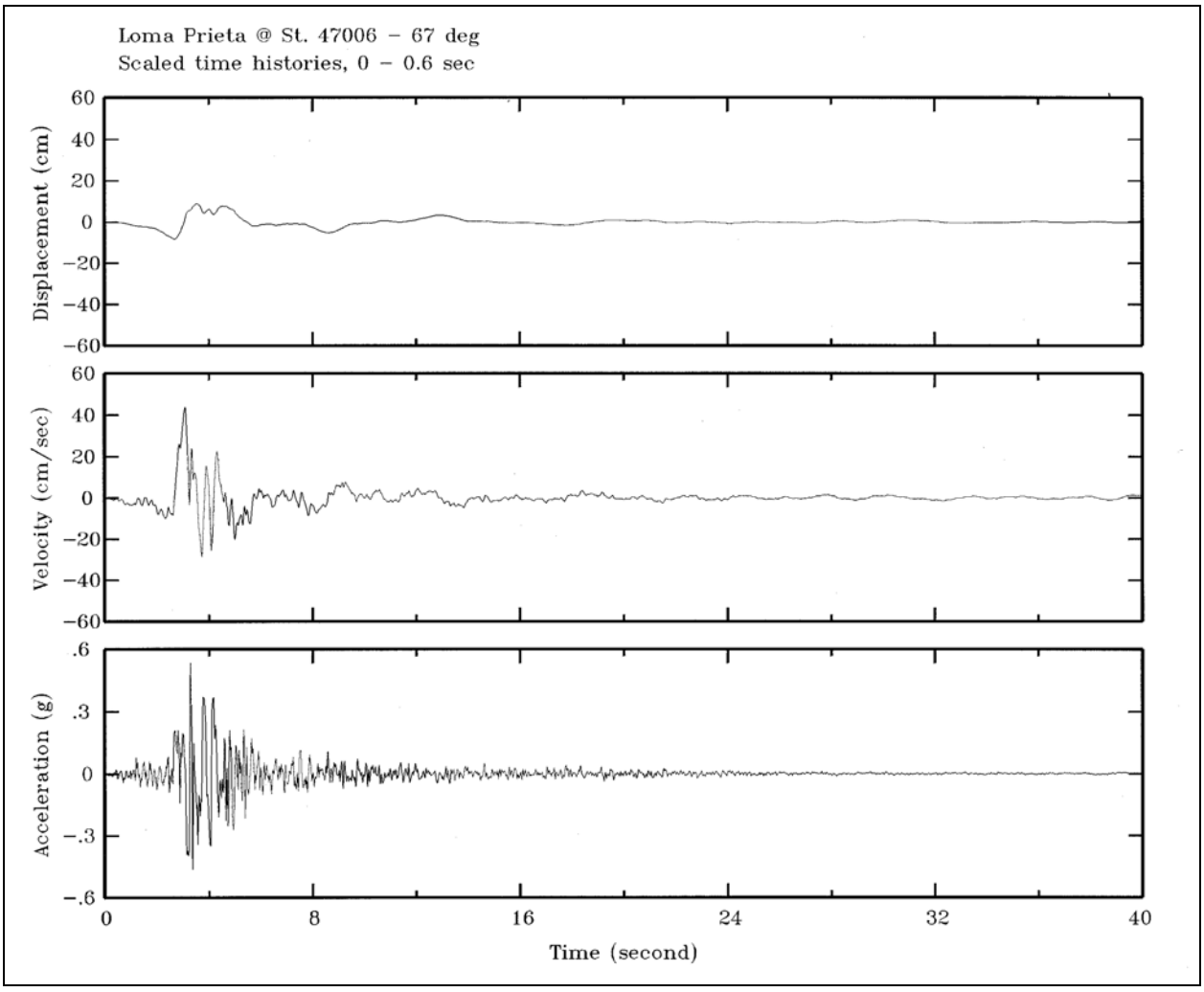

Figure D-5. Scaled time-histories of acceleration, velocity, and displacement for the 1989 Loma Prieta earthquake recorded at station 47006

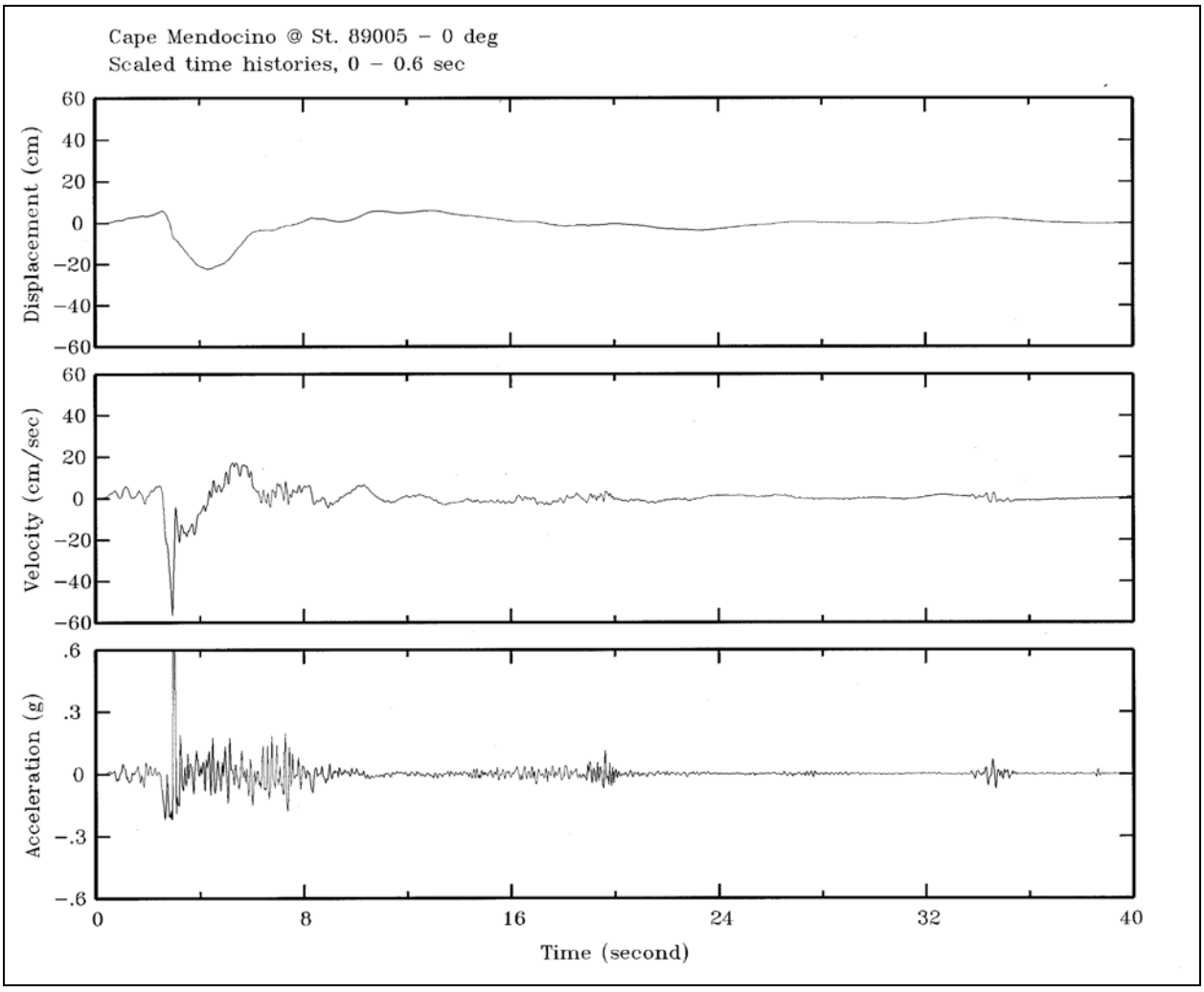

Figure D-6. Scaled time-histories of acceleration, velocity, and displacement for the 1992 Cape Mendocino earthquake recorded at station 89005

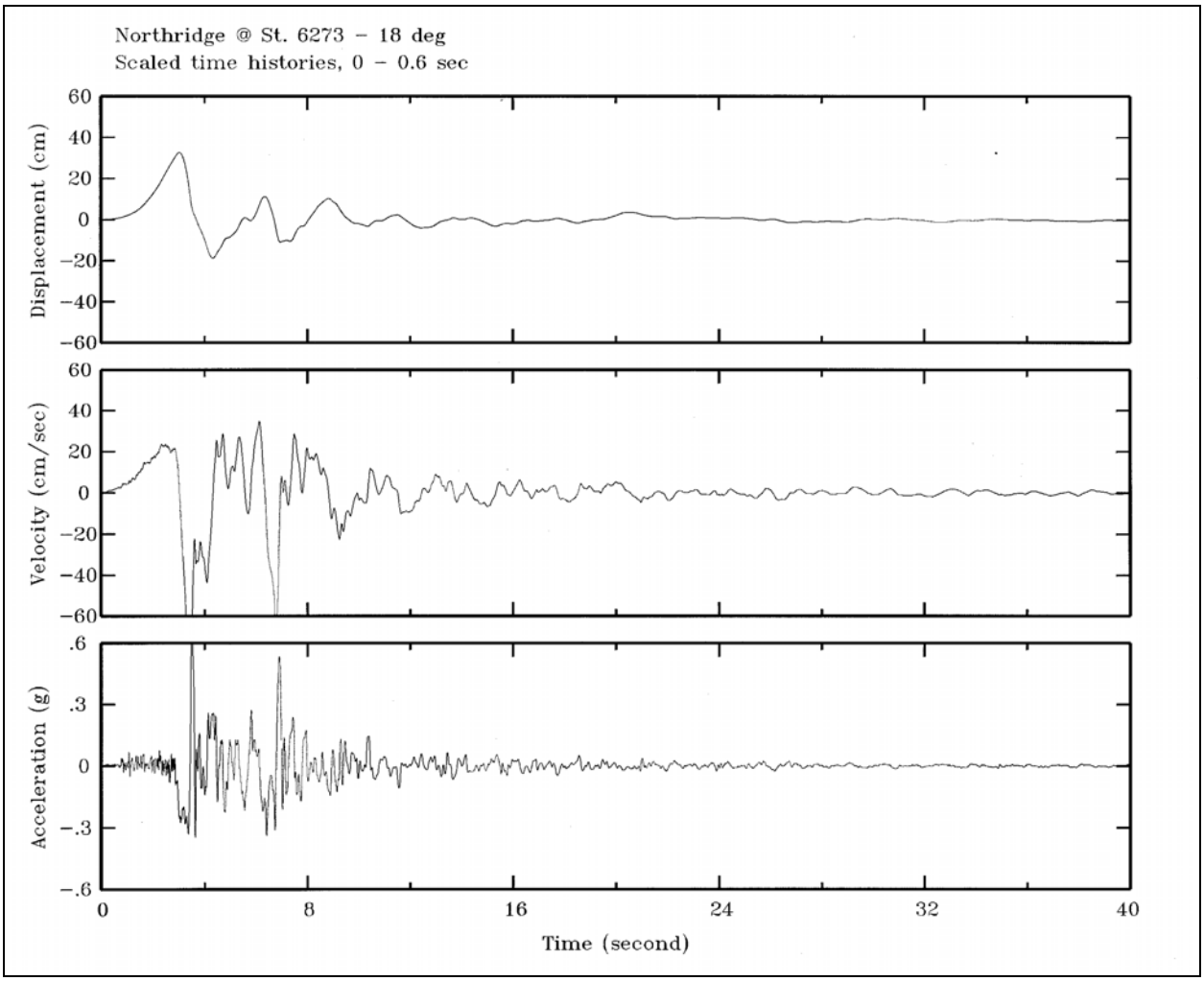

Figure D-7. Scaled time-histories of acceleration, velocity, and displacement for the 1994 Northridge earthquake recorded at station 6273

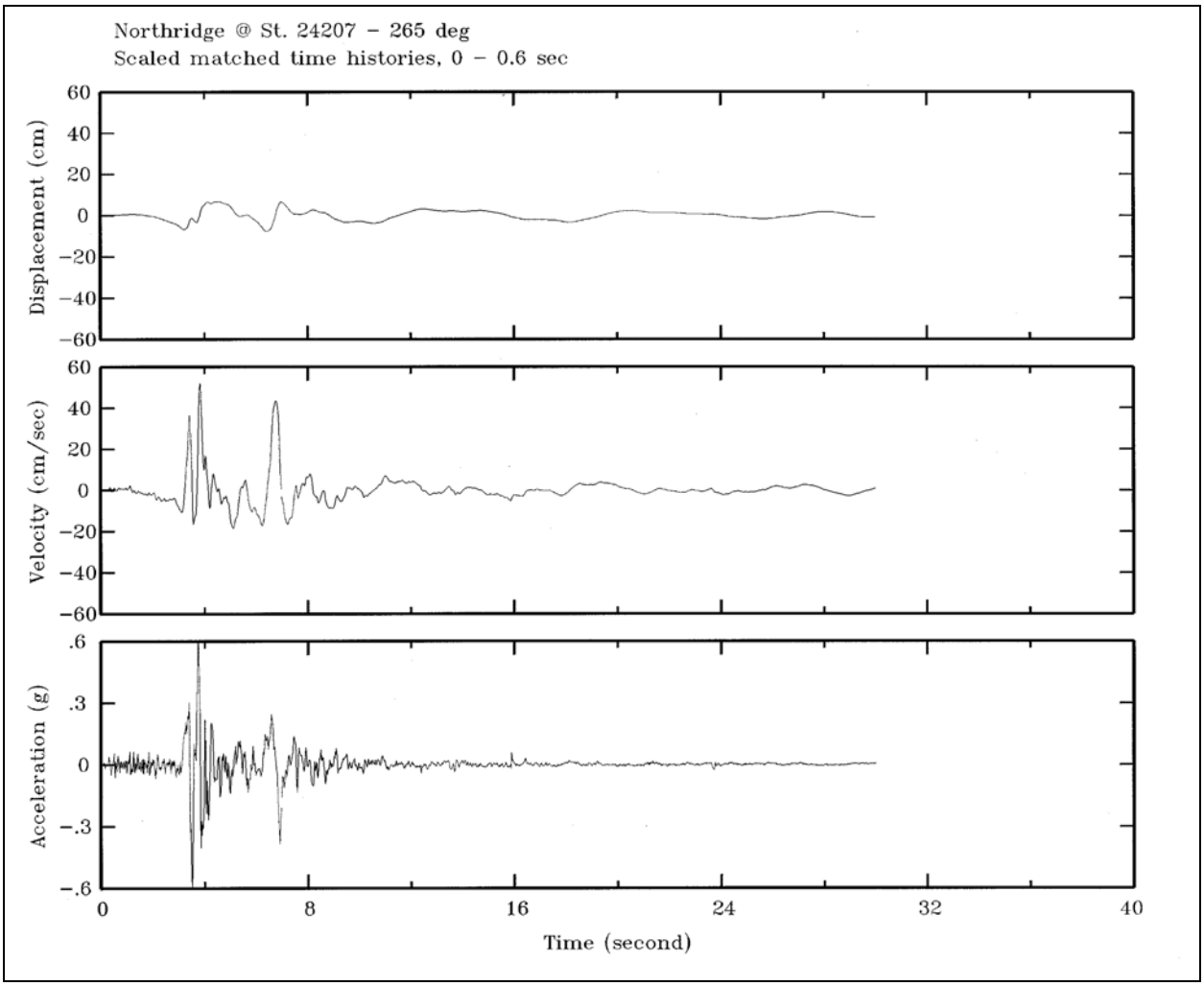

Figure D-8. Scaled time-histories of acceleration, velocity, and displacement for the 1994 Northridge earthquake recorded at station 24207

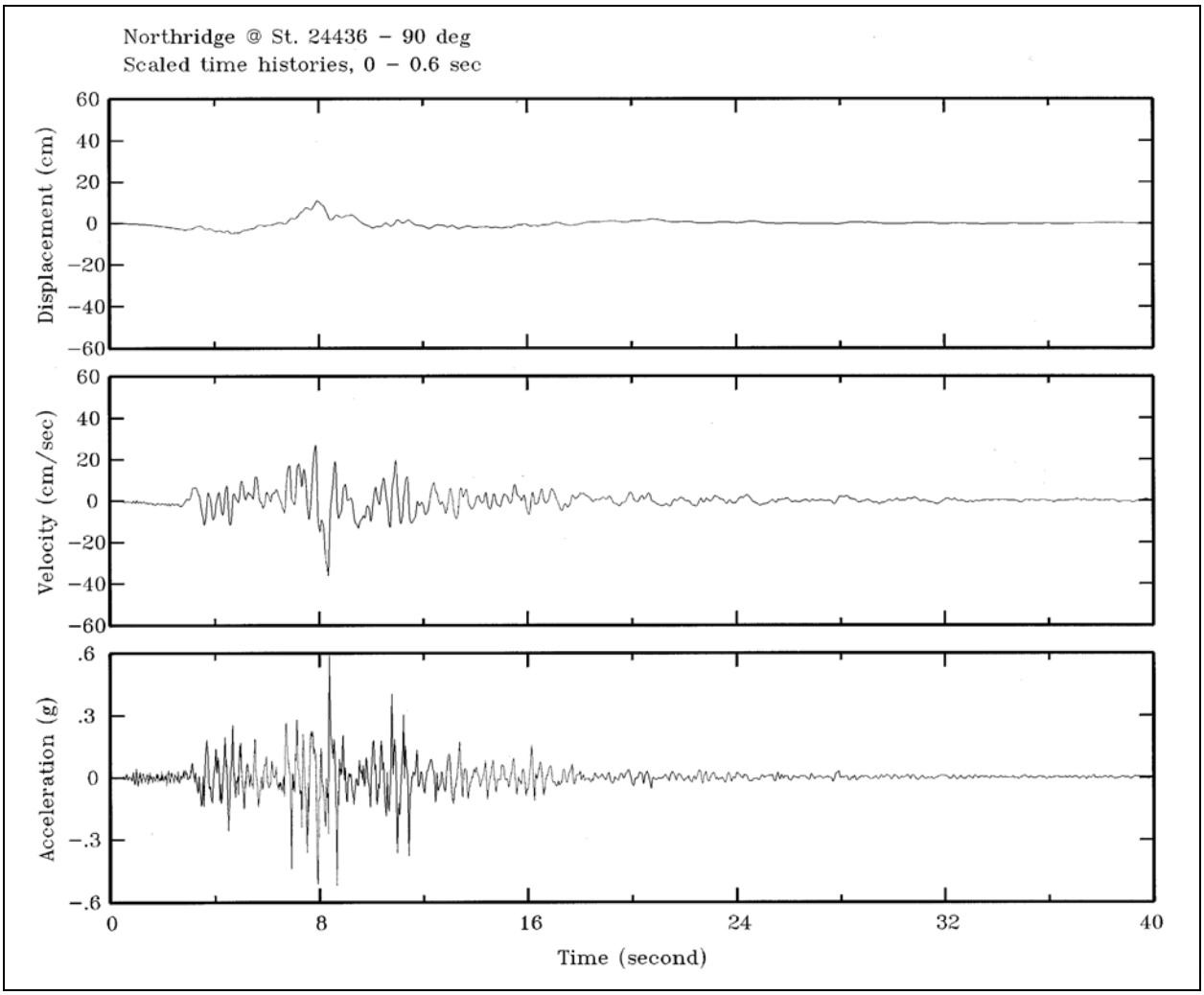

Figure D-9. Scaled time-histories of acceleration, velocity, and displacement for the 1994 Northridge earthquake recorded at station 24436

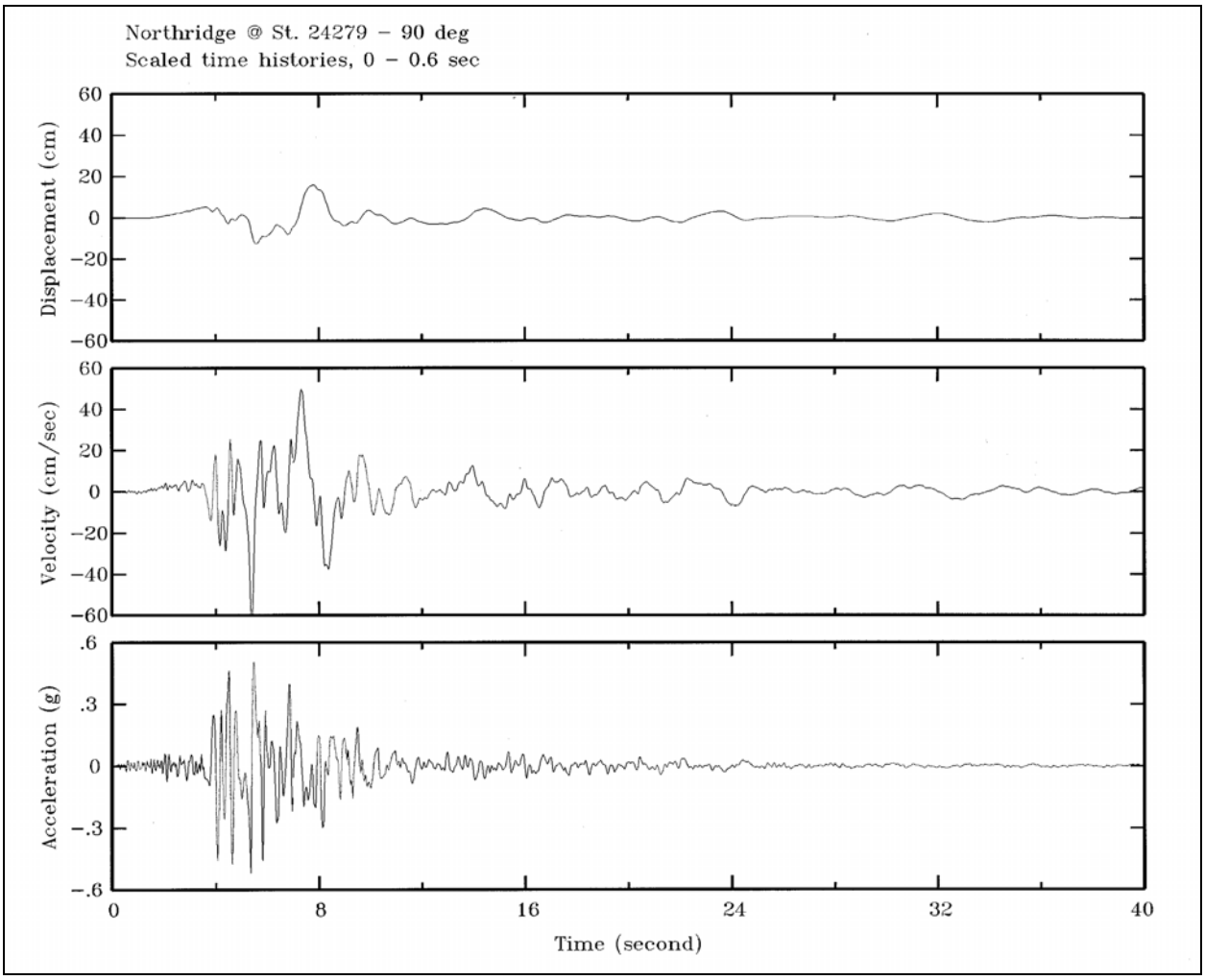

Figure D-10. Scaled time-histories of acceleration, velocity, and displacement for the 1994 Northridge earthquake recorded at station 24279

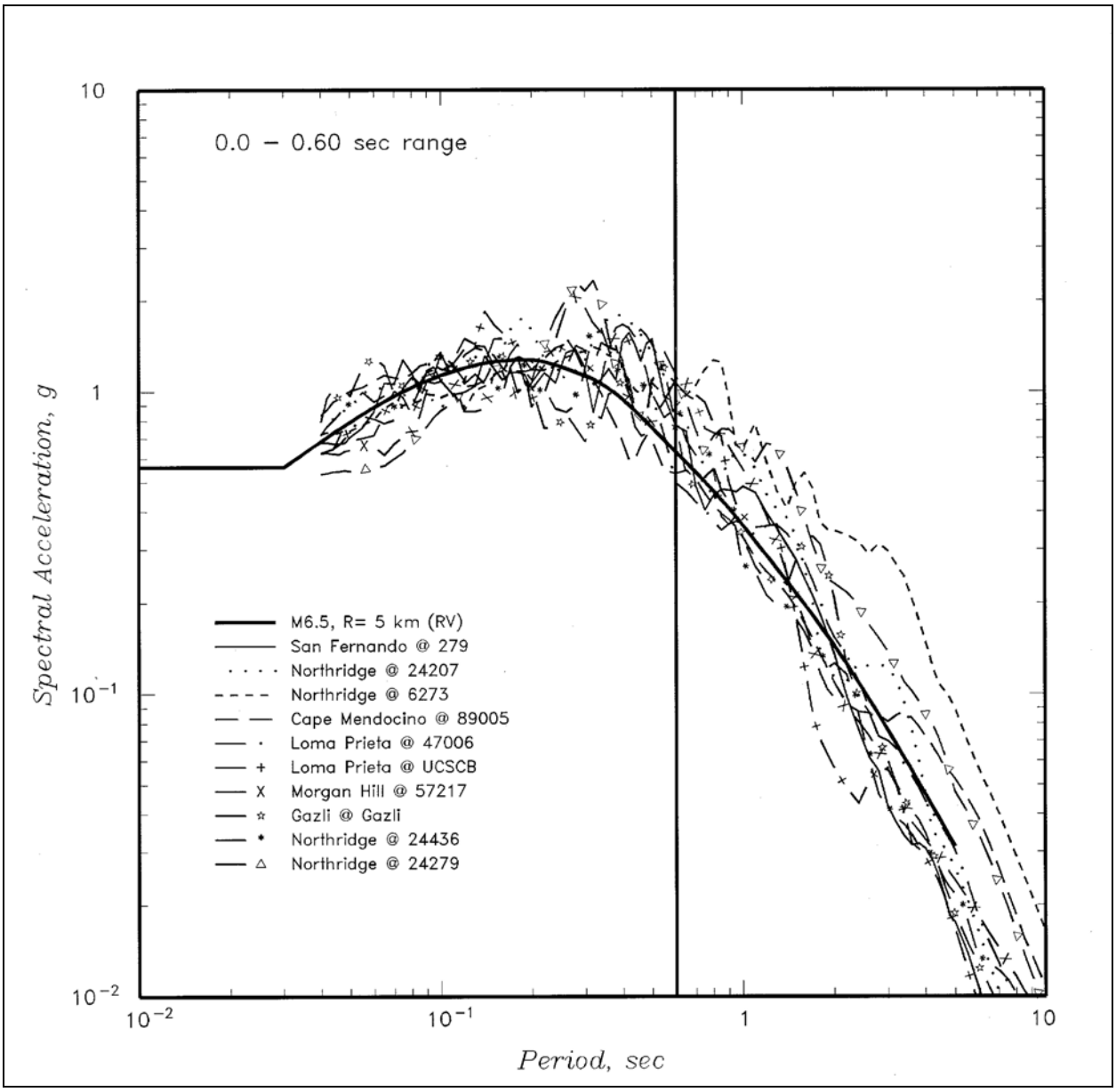

Figure D-11. Comparison of deterministic response spectrum and response spectra of scaled time-histories

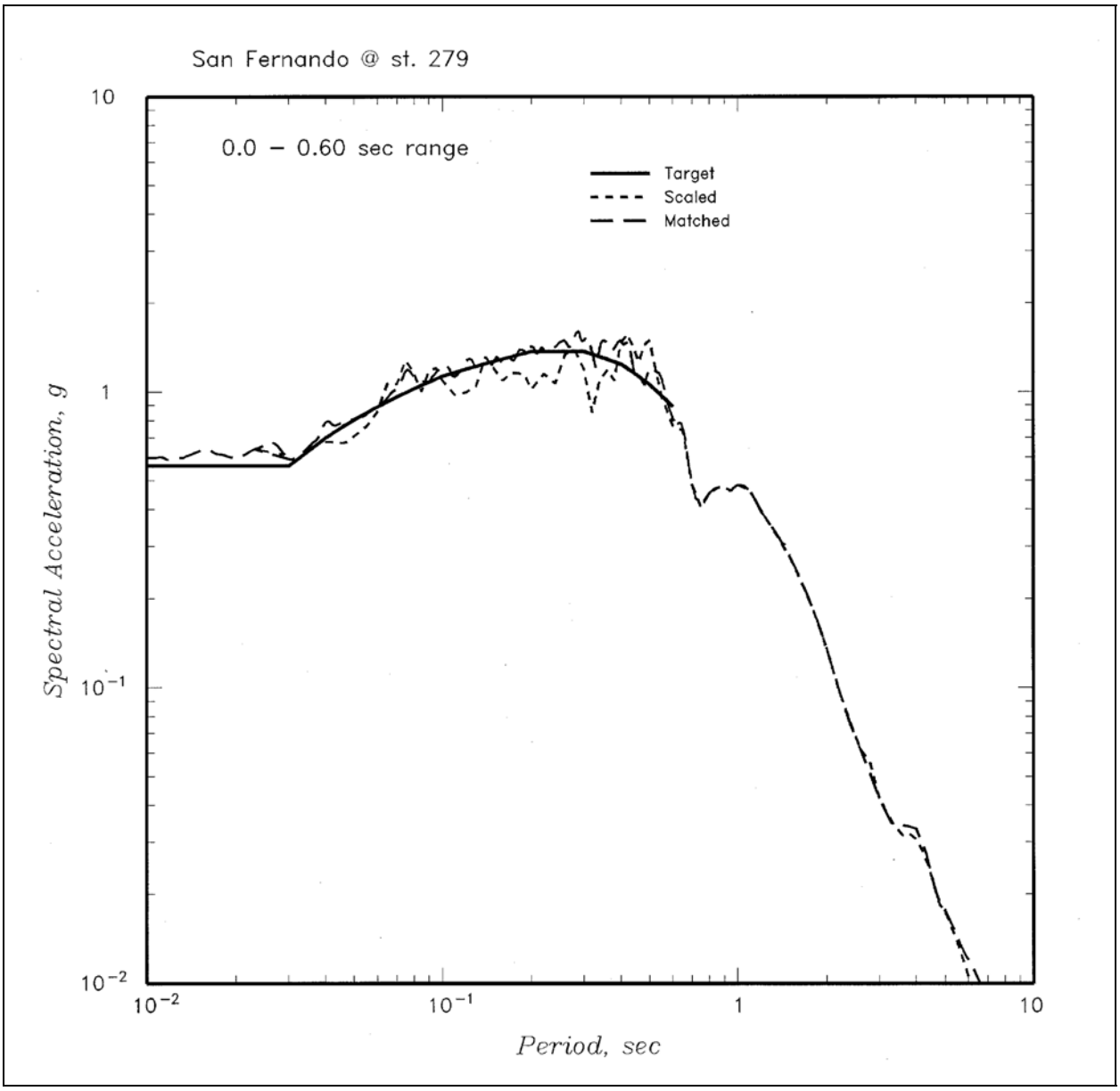

Figure D-12. Comparison of target spectrum and response spectra of time-history before and after spectral matching for the 1971 San Fernando earthquake recorded at station 279

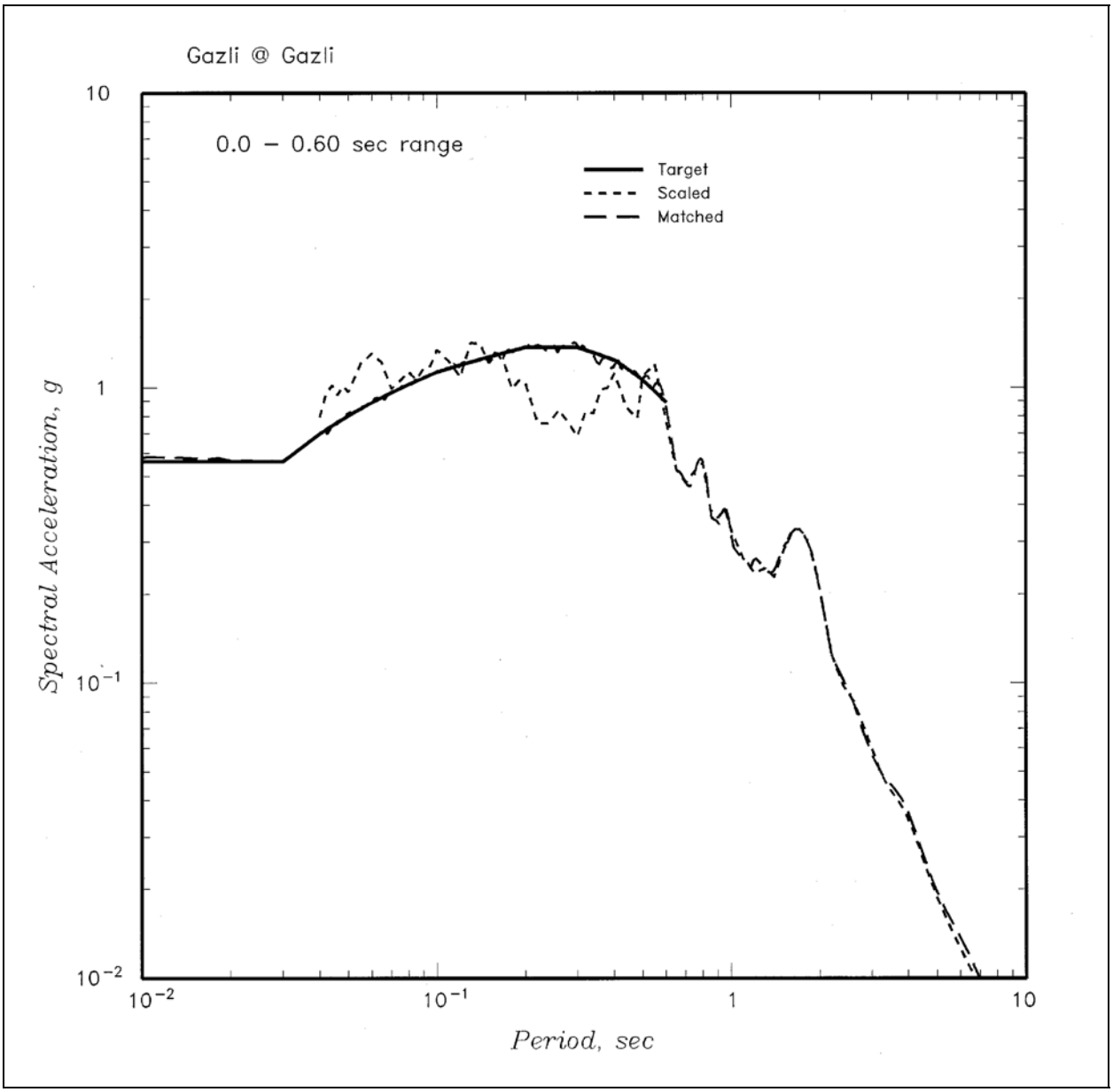

Figure D-13. Comparison of target spectrum and response spectra of time-history before and after spectral matching for the 1976 Gazli earthquake recorded at Gazli

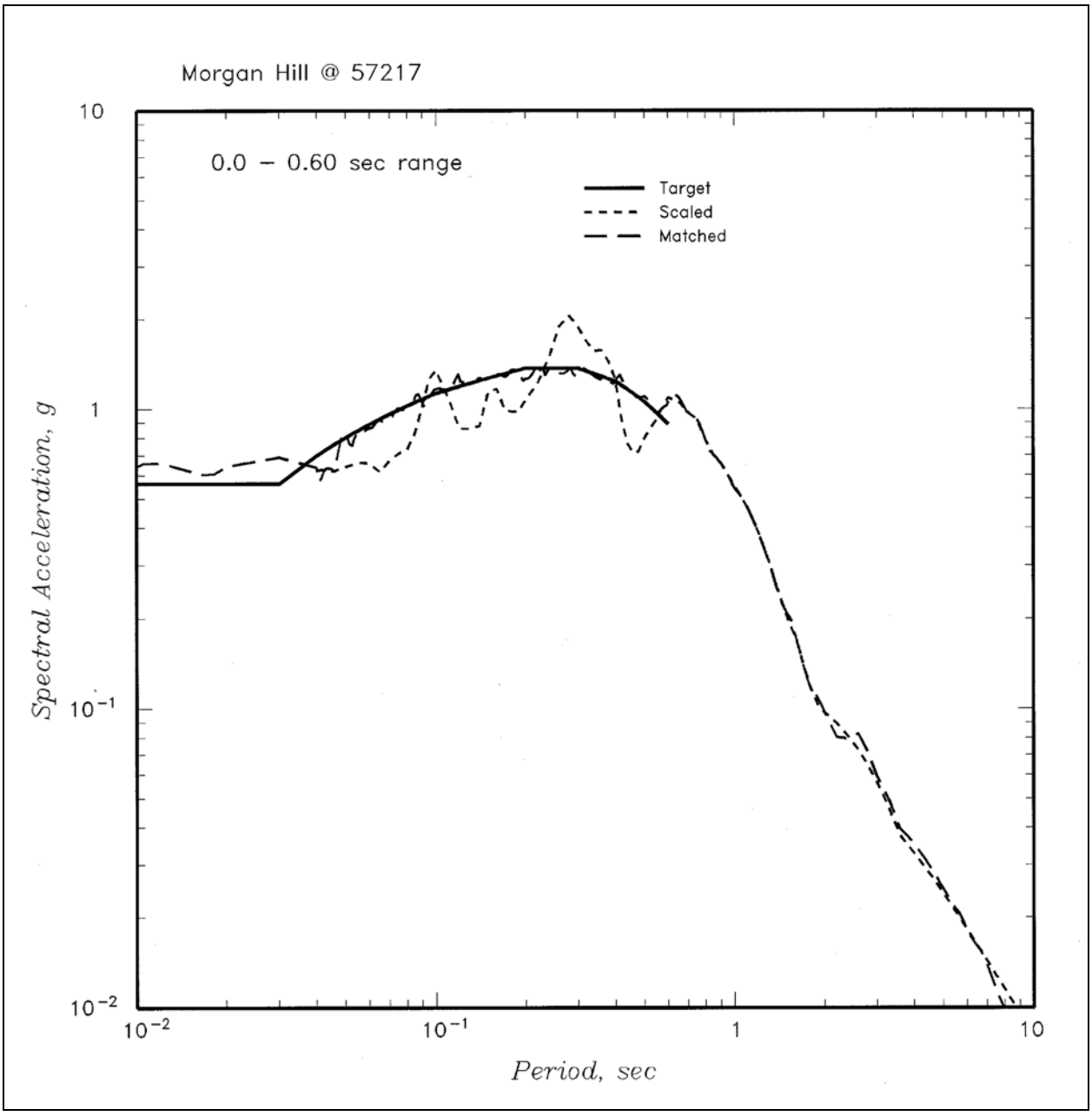

Figure D-14. Comparison of target spectrum and response spectra of time-history before and after spectral matching for the 1984 Morgan Hill earthquake recorded at station 57217

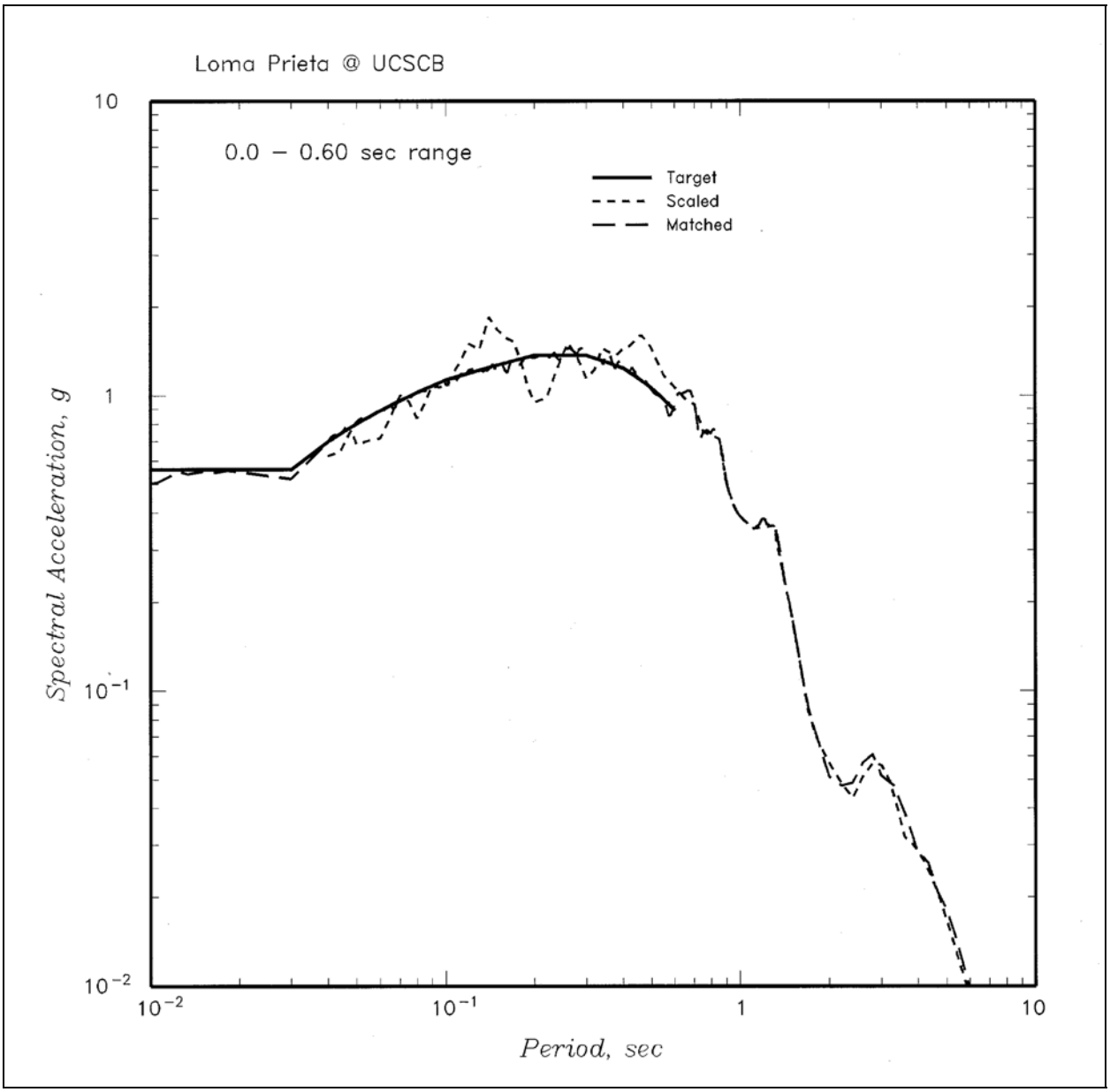

Figure D-15. Comparison of target spectrum and response spectra of time-history before and after spectral matching for the 1989 Loma Prieta earthquake recorded at UCSB Brane building

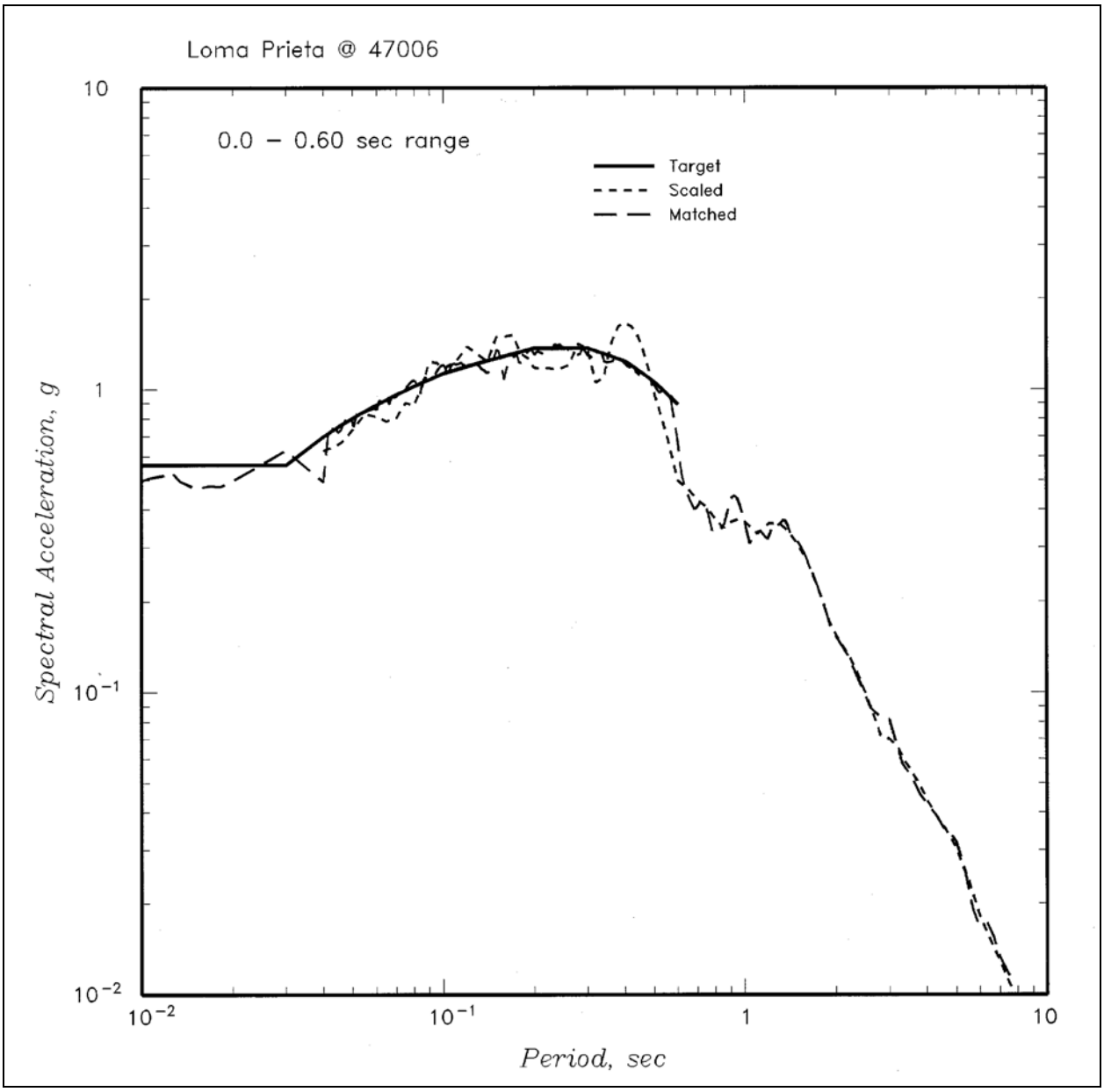

Figure D-16. Comparison of target spectrum and response spectra of time-history before and after spectral matching for the 1989 Loma Prieta earthquake recorded at station 47006

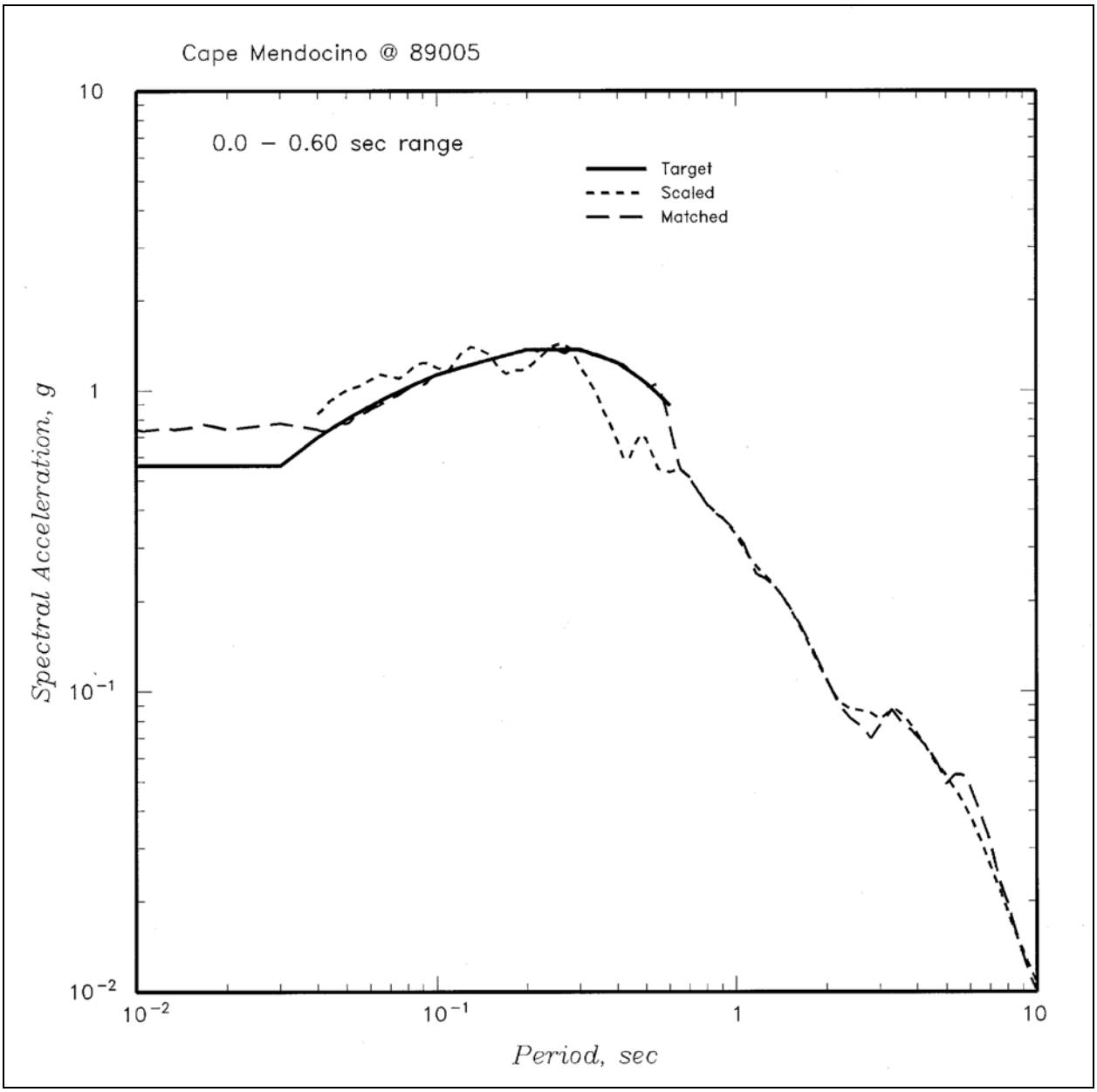

Figure D-17. Comparison of target spectrum and response spectra of time-history before and after spectral matching for the 1992 Cape Mendocino earthquake recorded at station 89005

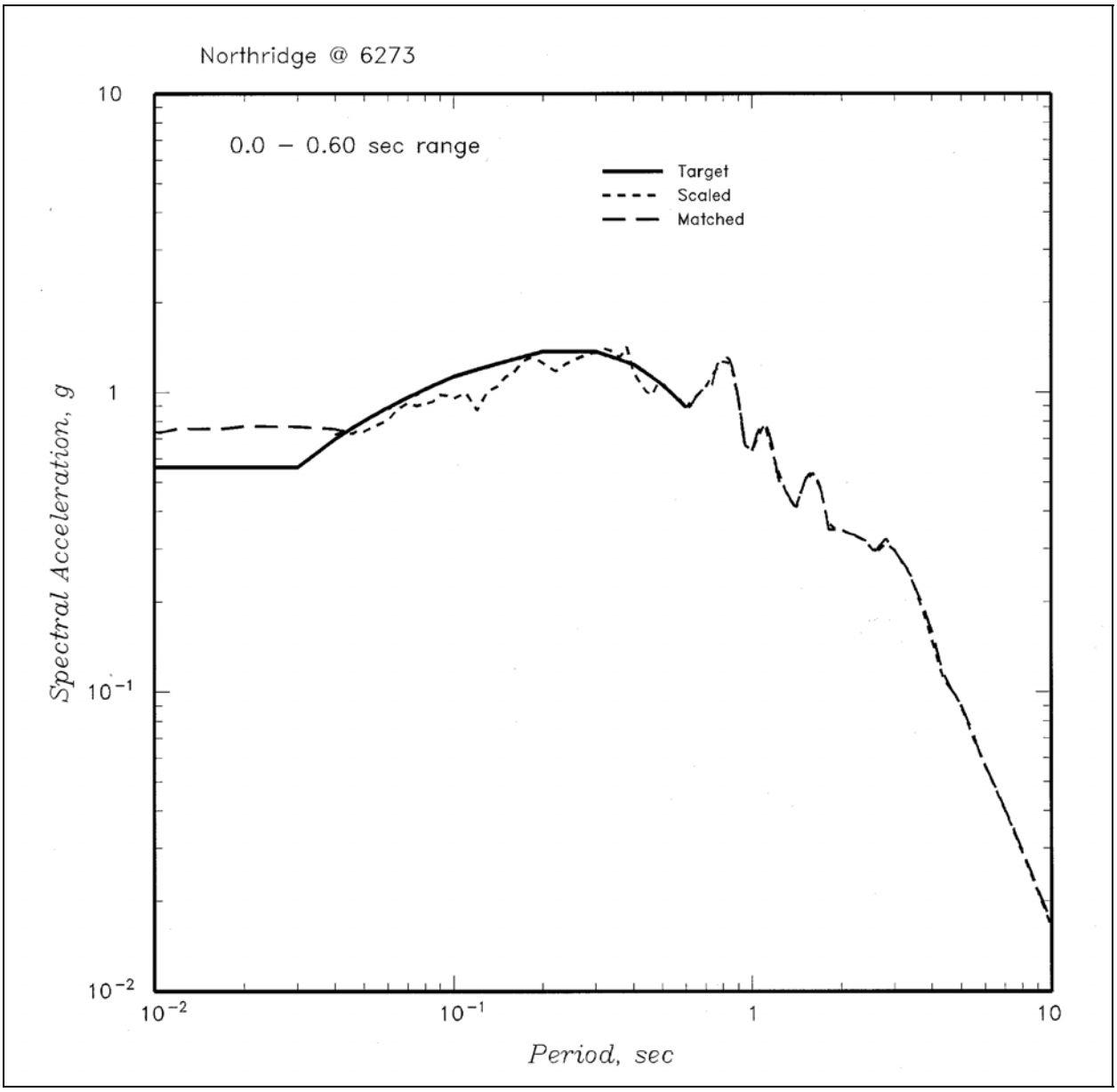

Figure D-18. Comparison of target spectrum and response spectra of time-history before and after spectral matching for the 1994 Northridge earthquake recorded at station 6273

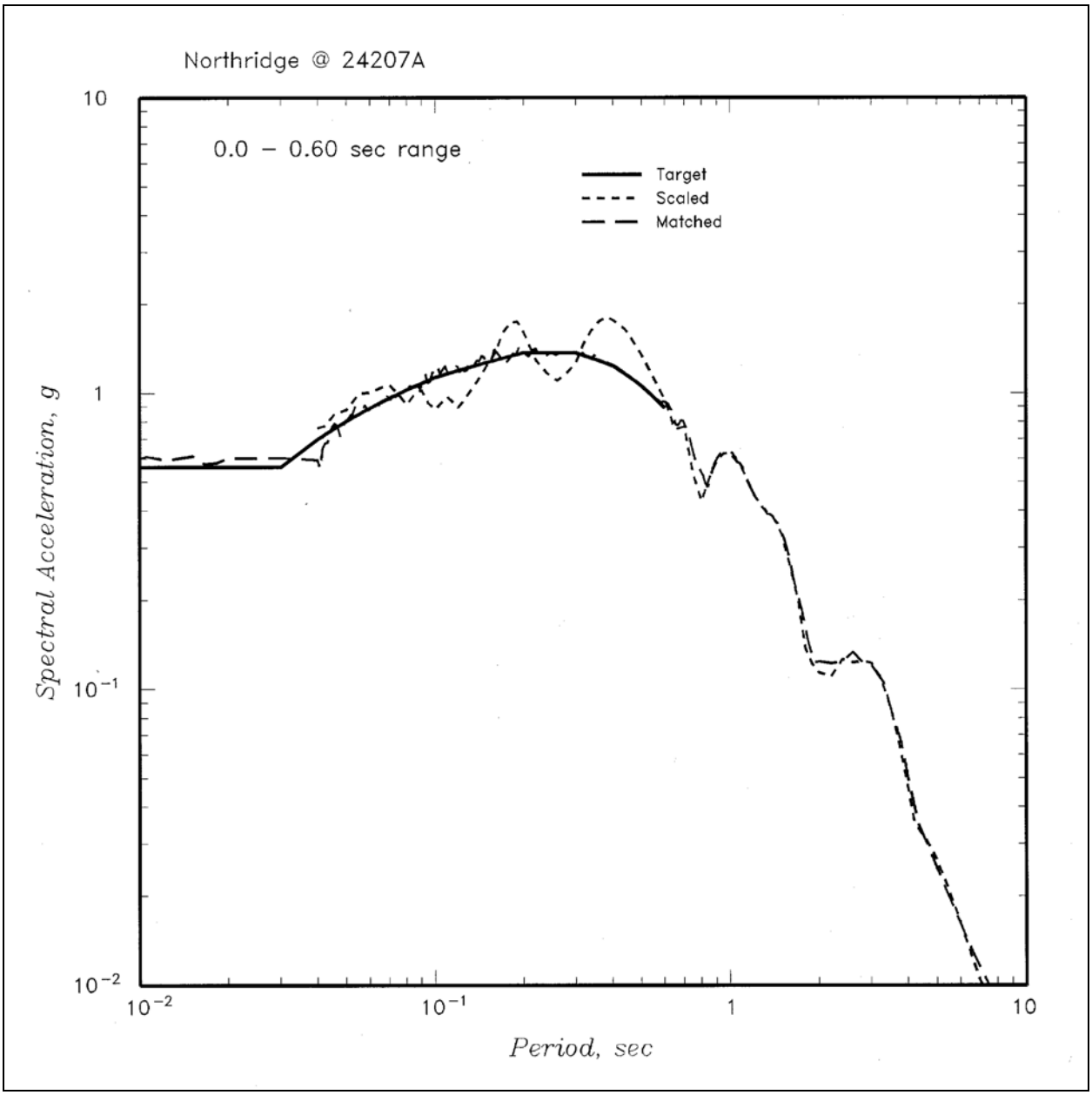

Figure D-19. Comparison of target spectrum and response spectra of time-history before and after spectral matching for the 1994 Northridge earthquake recorded at station 24207

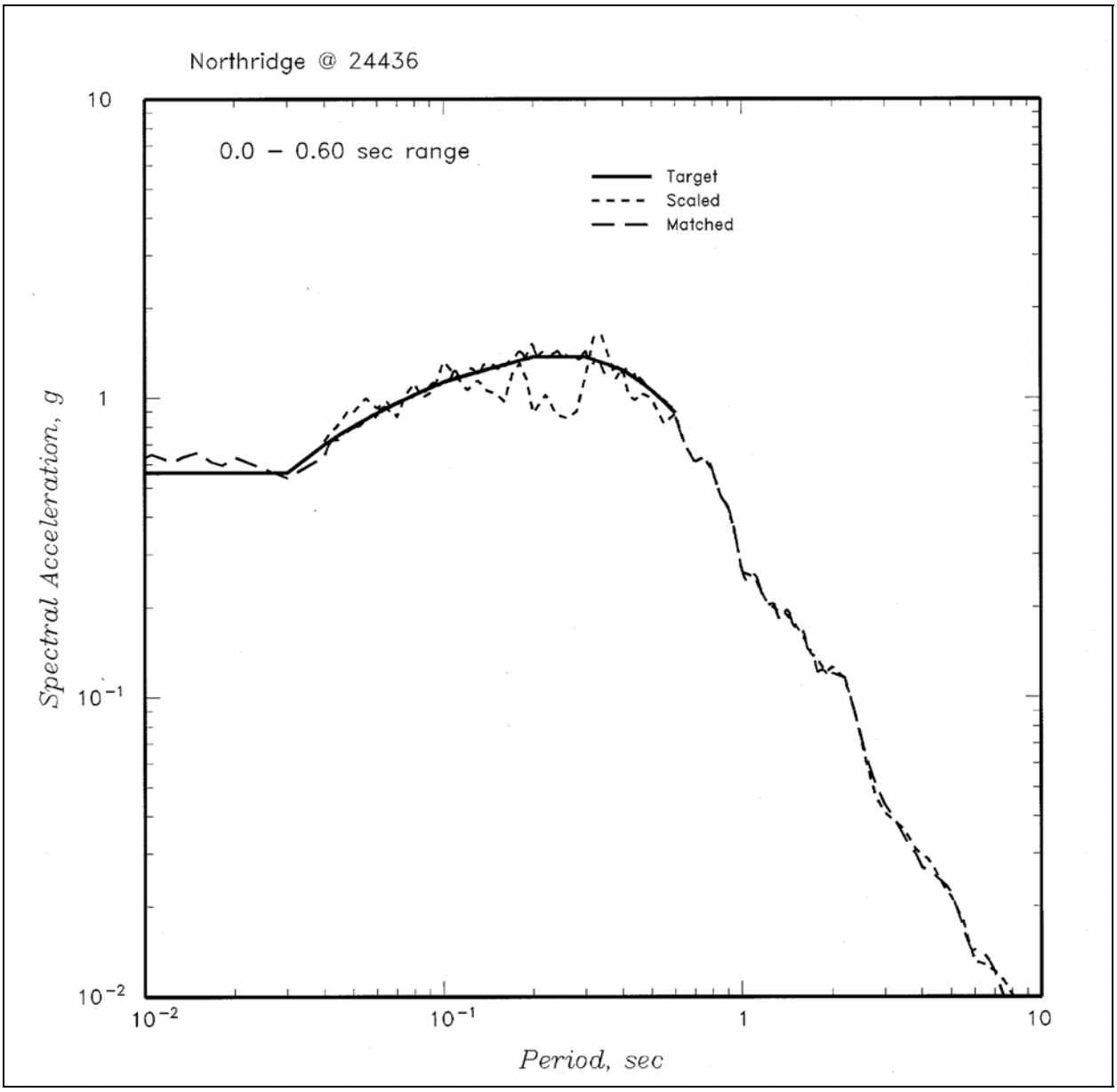

Figure D-20. Comparison of target spectrum and response spectra of time-history before and after spectral matching for the 1994 Northridge earthquake recorded at station 24436

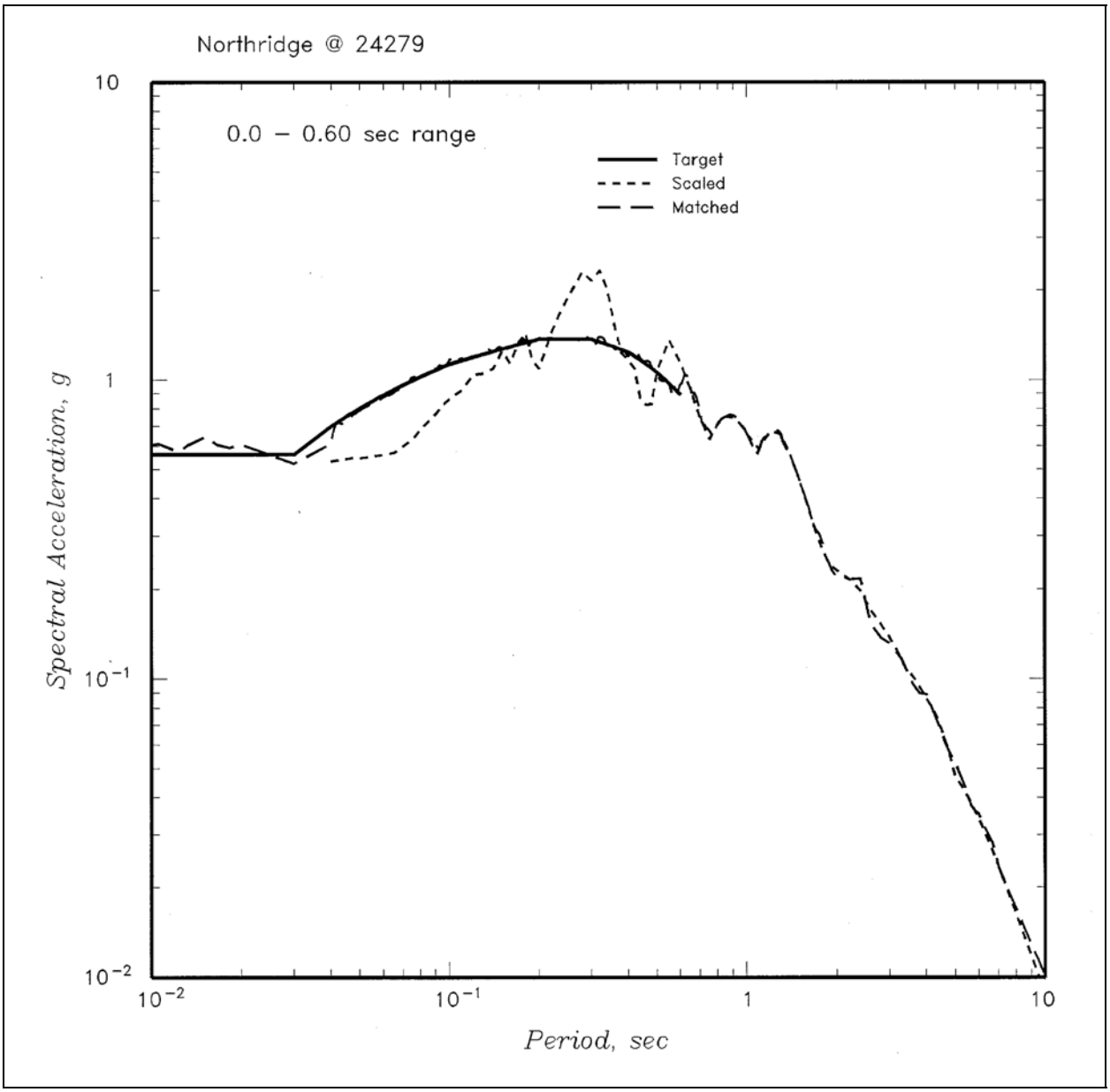

Figure D-21. Comparison of target spectrum and response spectra of time-history before and after spectral matching for the 1994 Northridge earthquake recorded at station 24279

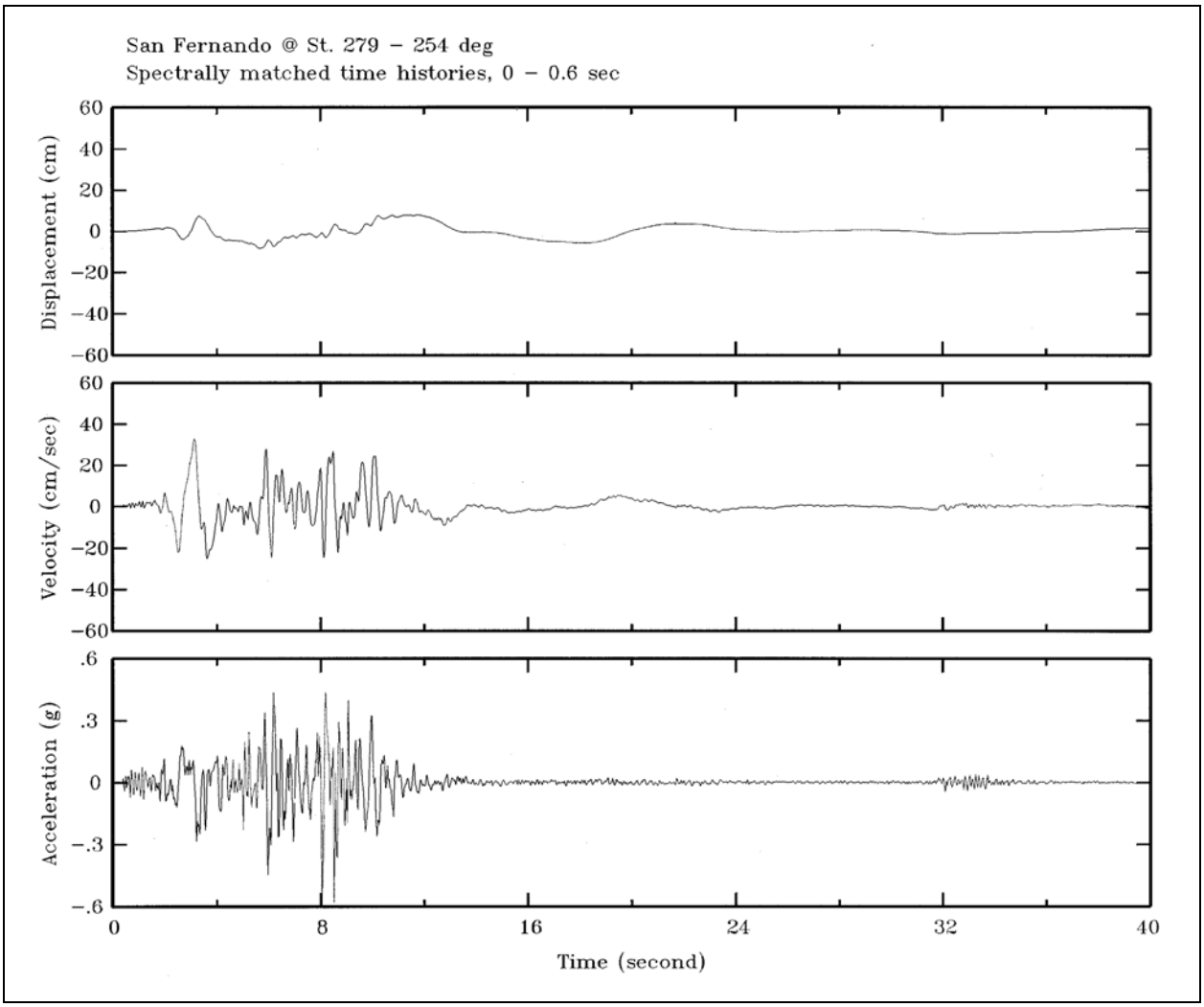

Figure D-22. Spectrally matched time-histories of acceleration, velocity, and displacement for the 1971 San Fernando earthquake recorded at station 279

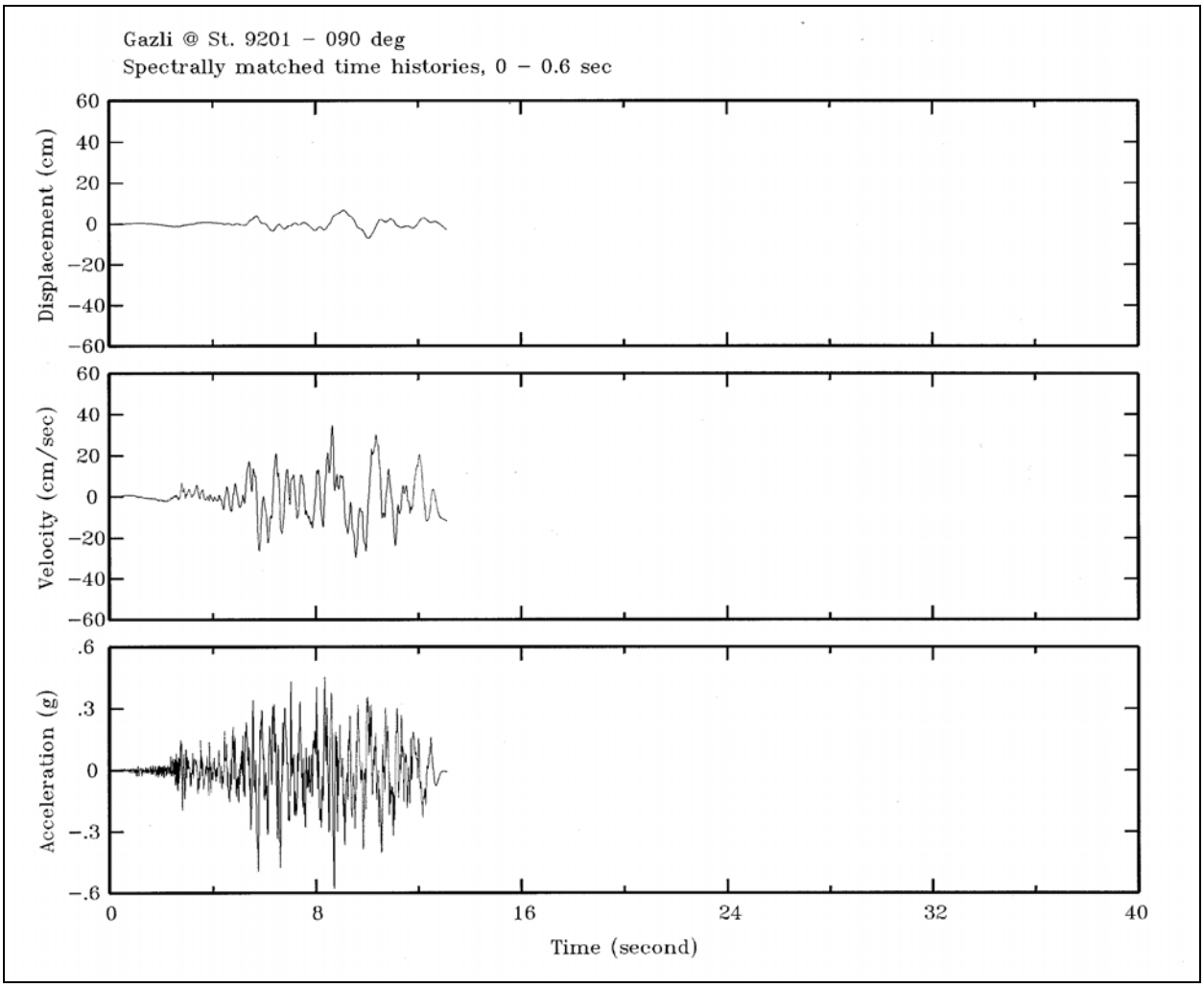

Figure D-23. Spectrally matched time-histories of acceleration, velocity, and displacement for the 1976 Gazli earthquake recorded at Gazli

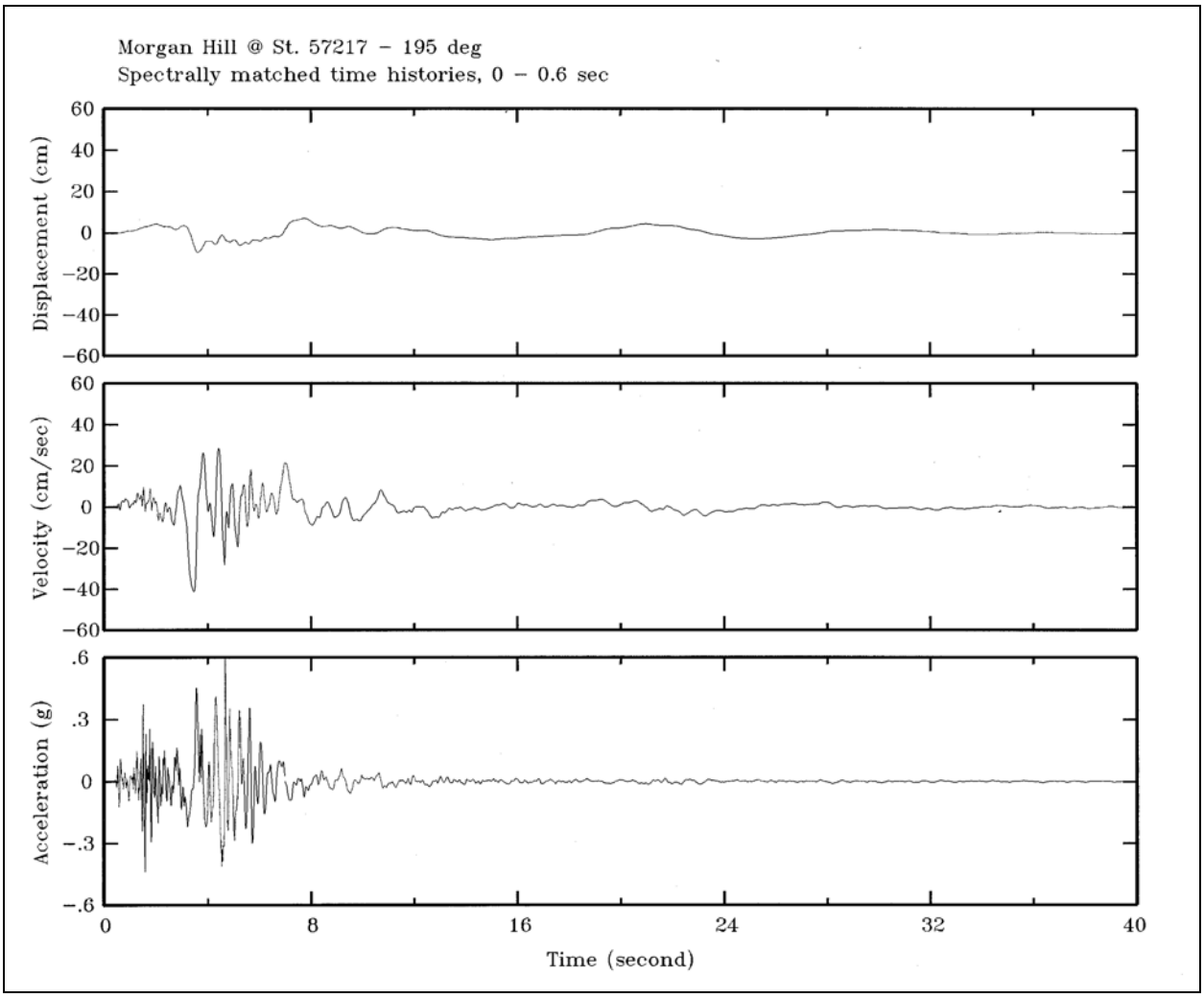

Figure D-24. Spectrally matched time-histories of acceleration, velocity, and displacement for the 1984 Morgan Hill earthquake recorded at station 57217

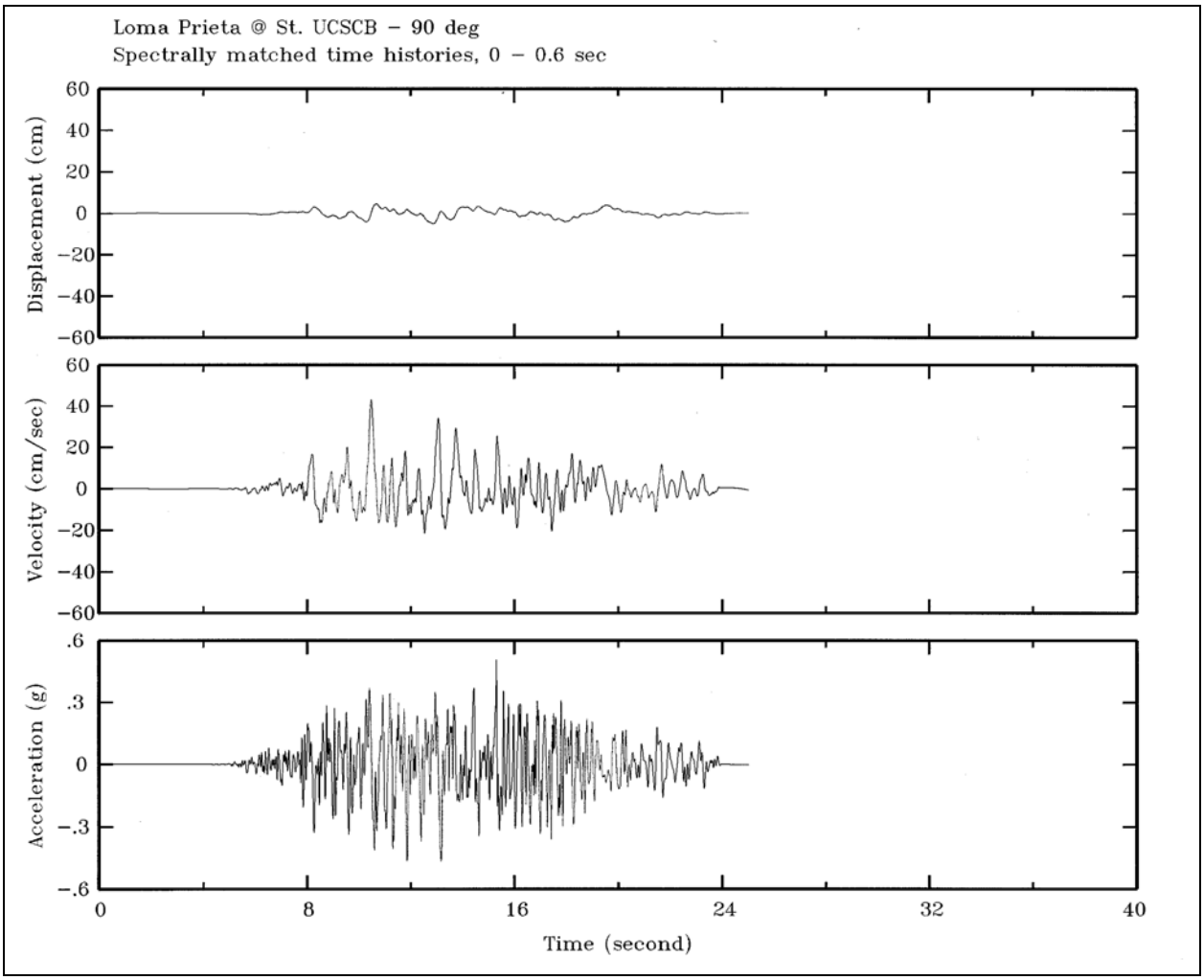

Figure D-25. Spectrally matched time-histories of acceleration, velocity, and displacement for the 1989 Loma Prieta earthquake recorded at UCSC Brane building

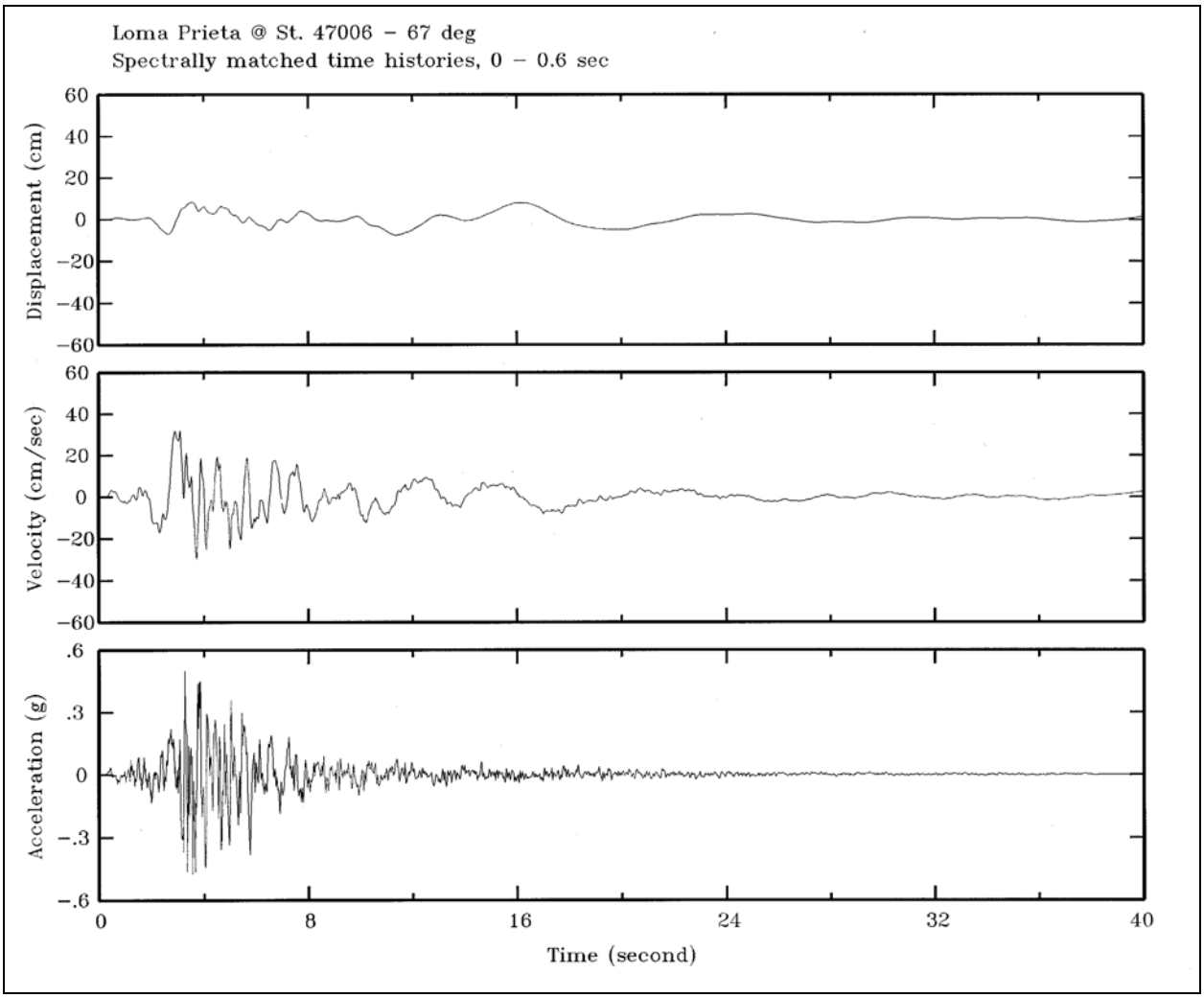

Figure D-26. Spectrally matched time-histories of acceleration, velocity, and displacement for the 1989 Loma Prieta earthquake recorded at station 47006

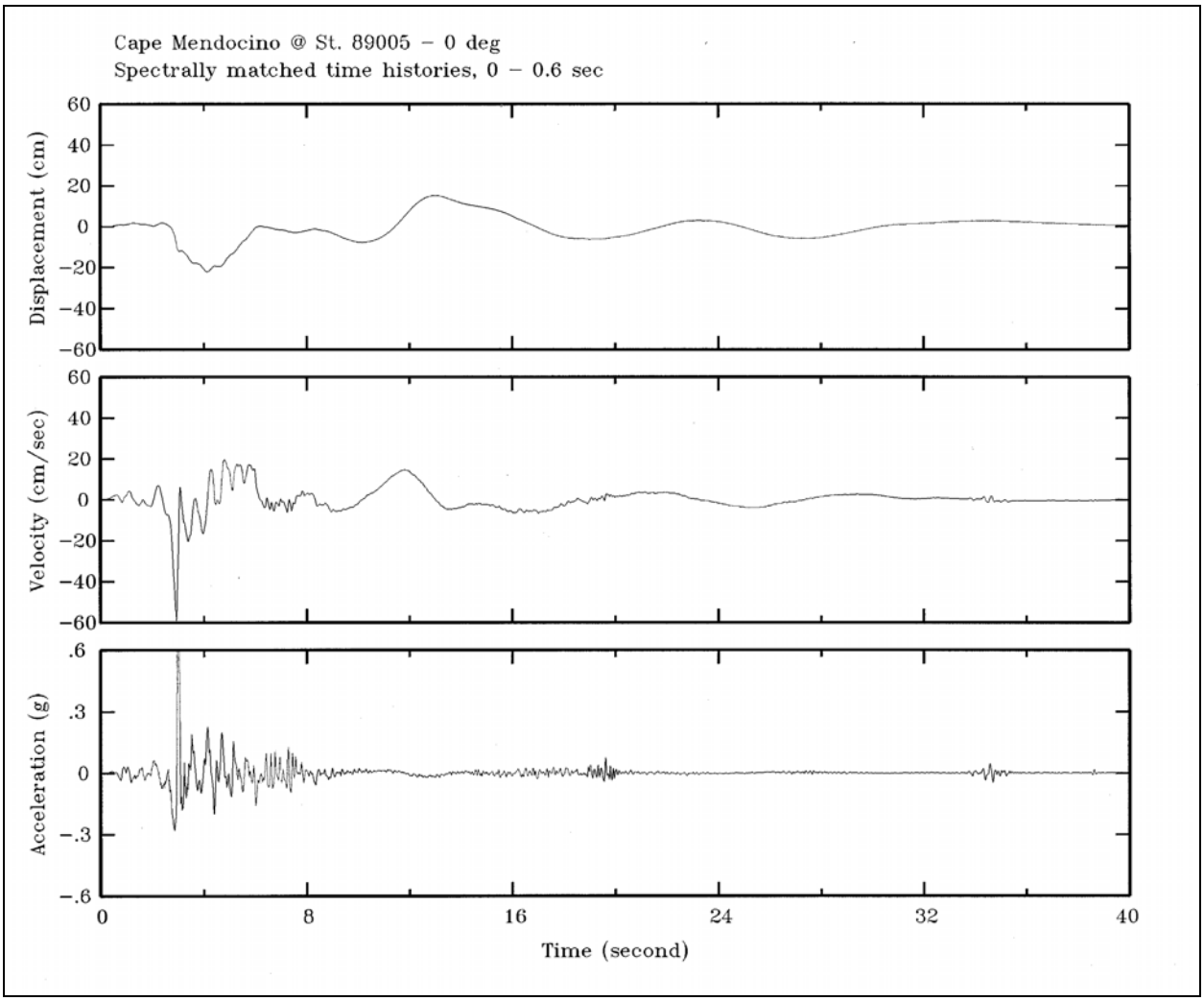

Figure D-27. Spectrally matched time-histories of acceleration, velocity, and displacement for the 1992 Cape Mendocino earthquake recorded at station 89005

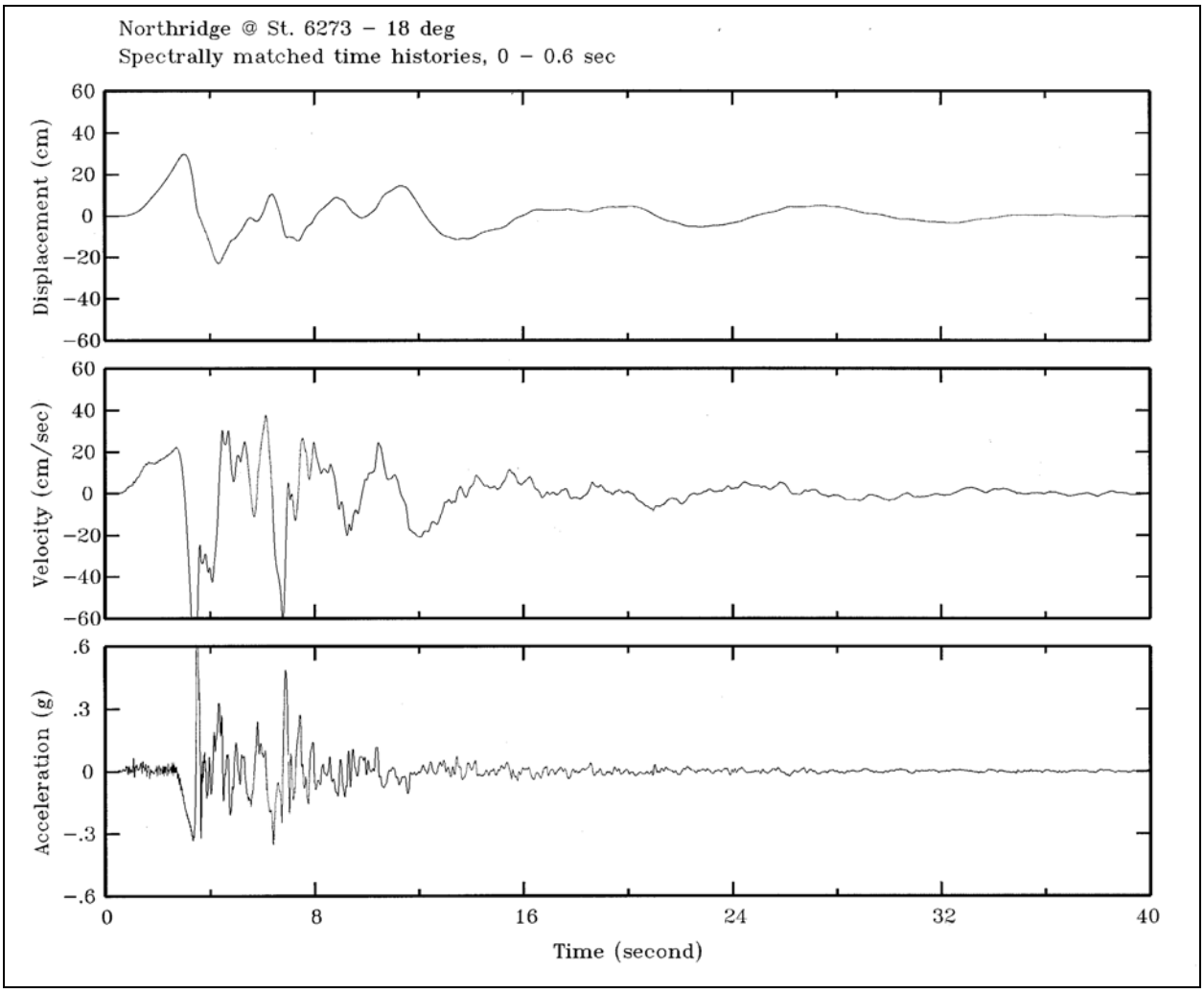

Figure D-28. Spectrally matched time-histories of acceleration, velocity, and displacement for the 1994 Northridge earthquake recorded at station 6273

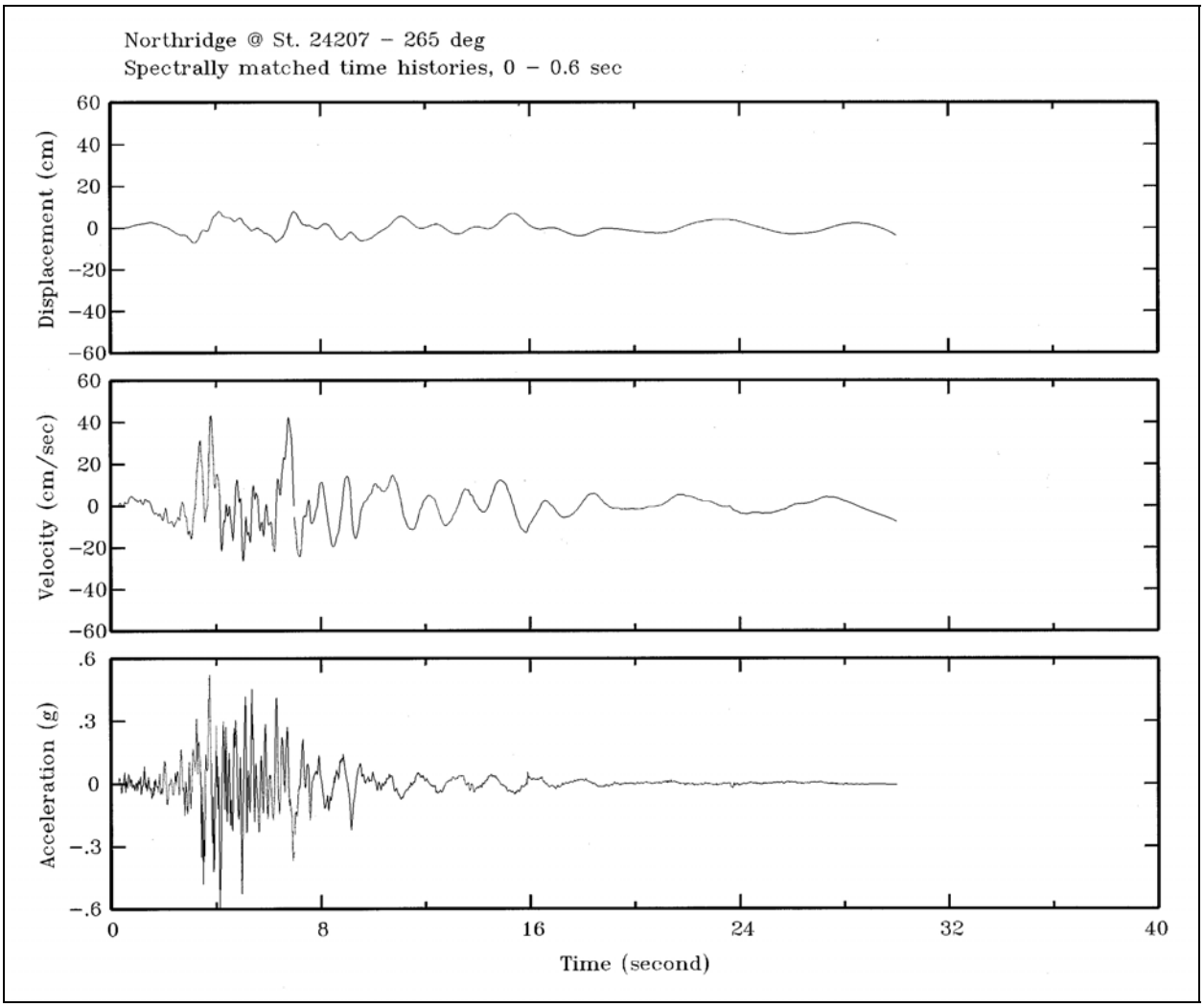

Figure D-29. Spectrally matched time-histories of acceleration, velocity, and displacement for the 1994 Northridge earthquake recorded at station 24207

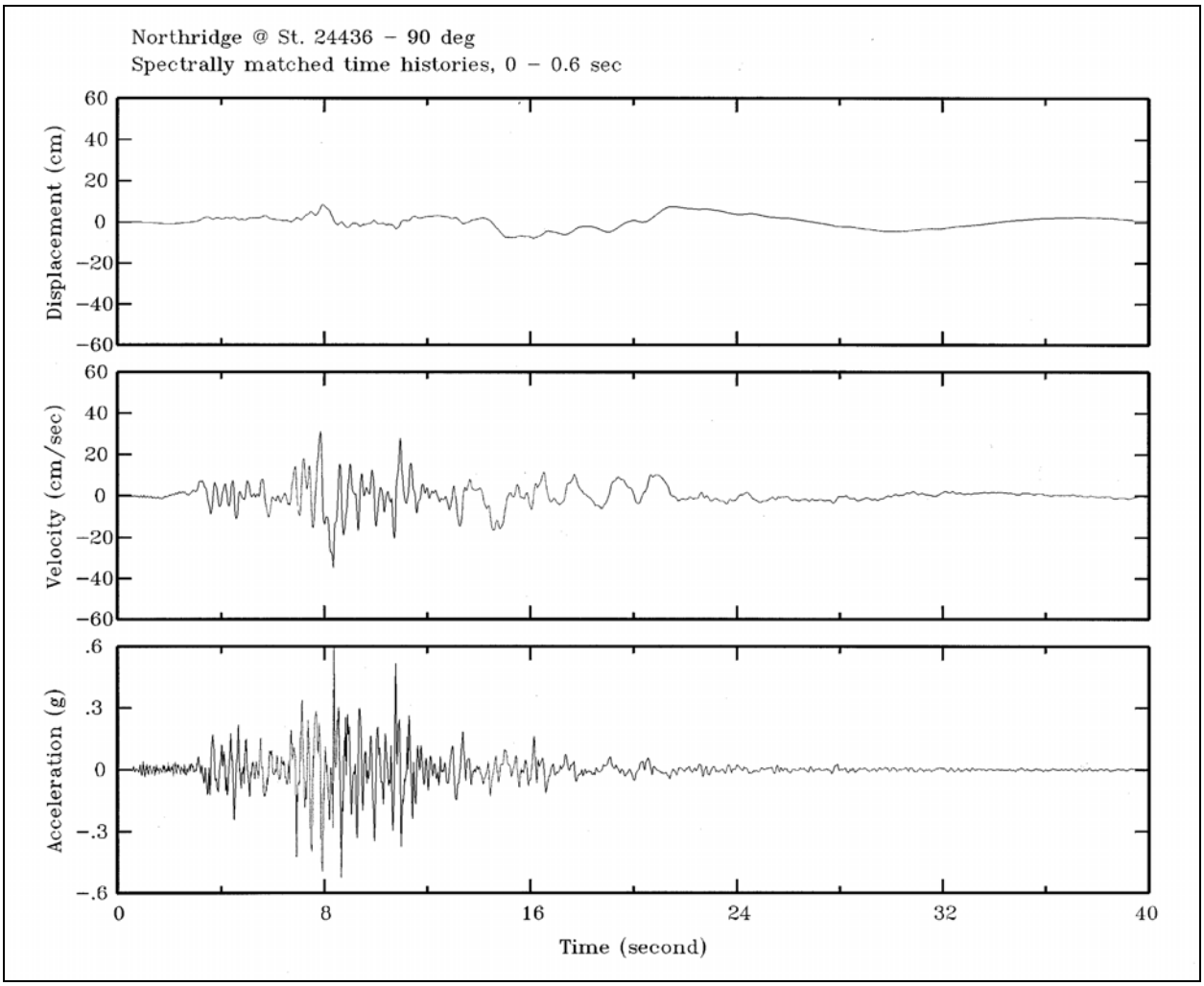

Figure D-30. Spectrally matched time-histories of acceleration, velocity, and displacement for the 1994 Northridge earthquake recorded at station 24436

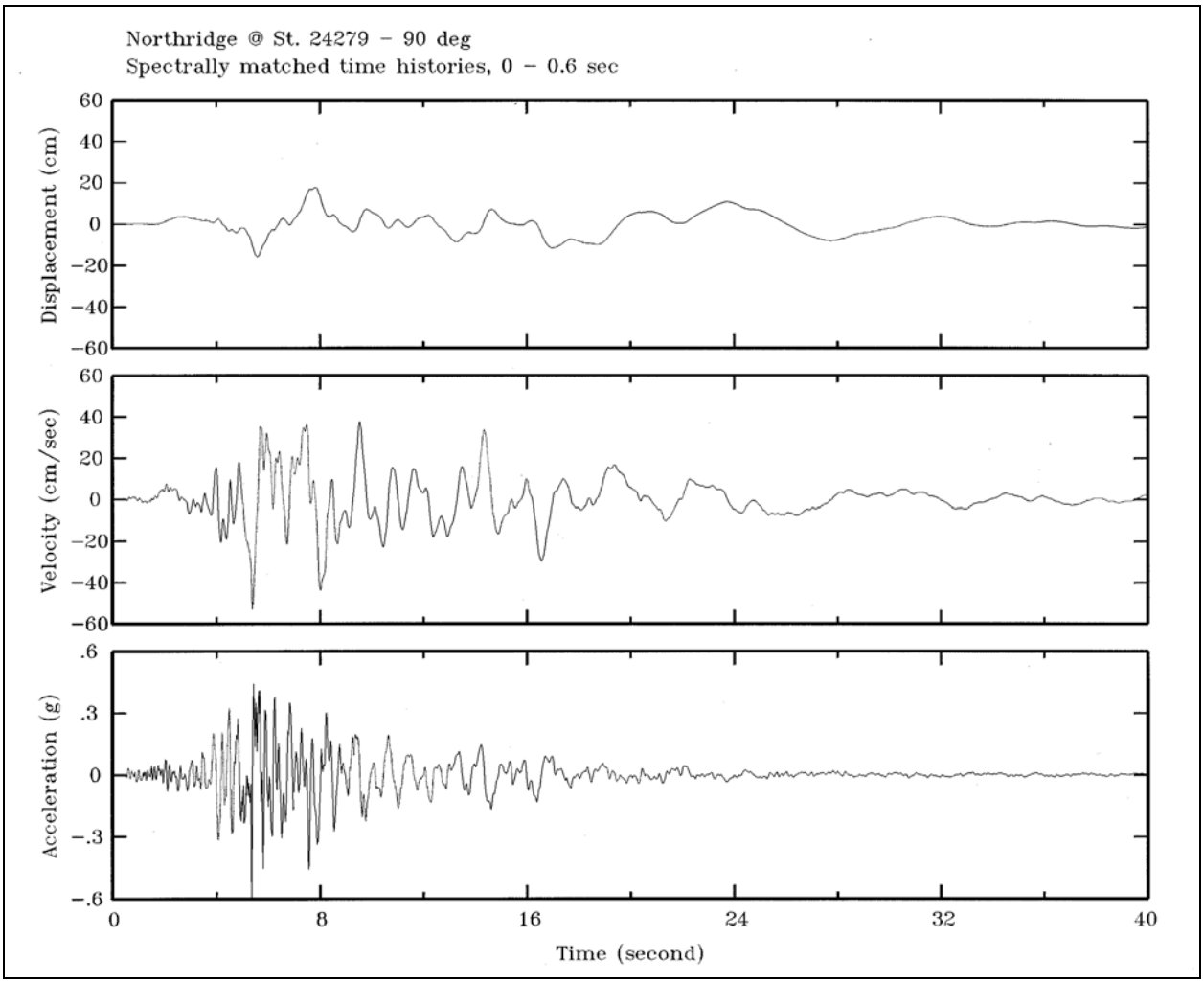

Figure D-31. Spectrally matched time-histories of acceleration, velocity, and displacement for the 1994 Northridge earthquake recorded at station 24279

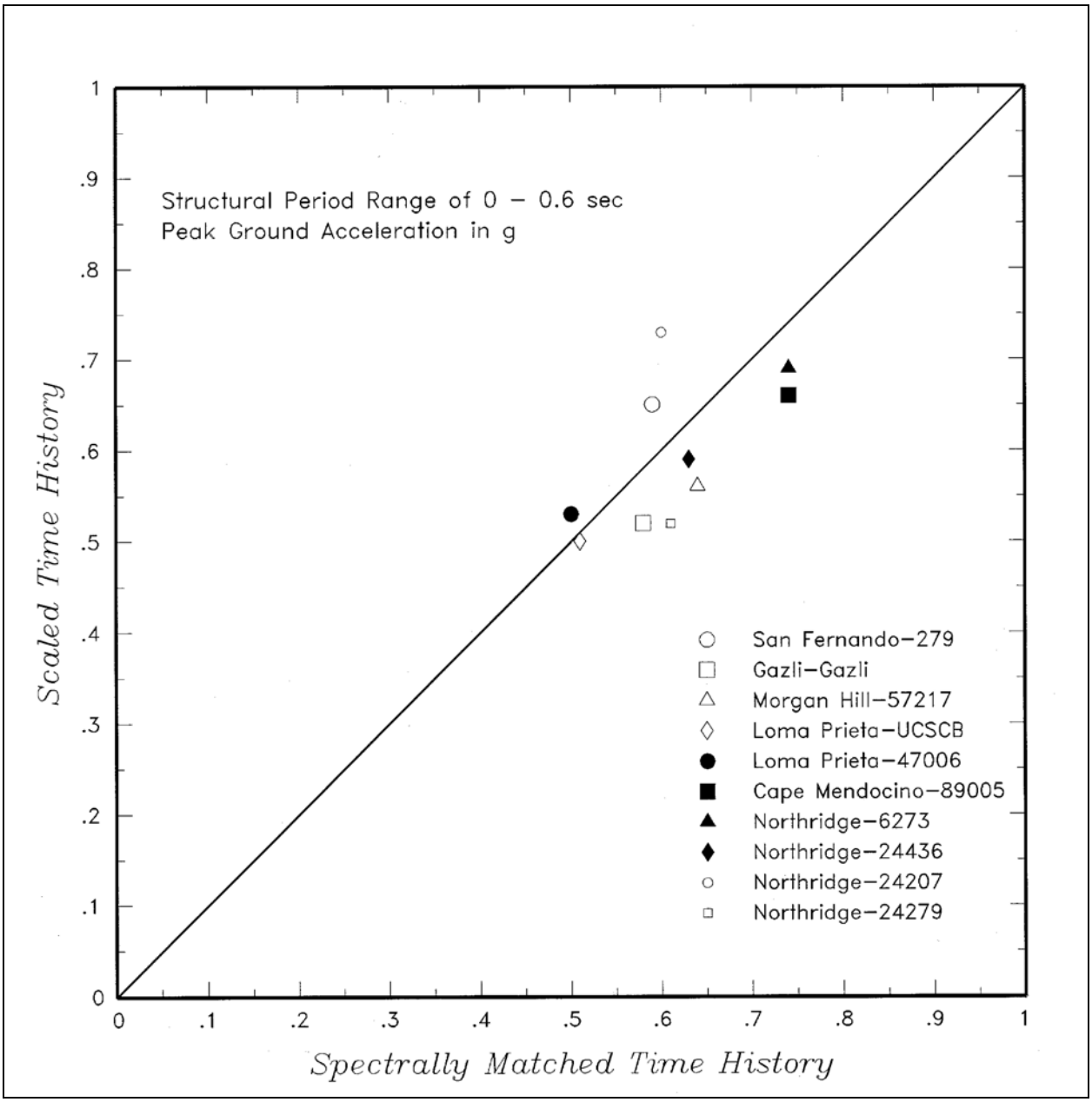

Figure D-32. Comparison for peak ground acceleration estimated from the scaled and spectrally matched time-histories

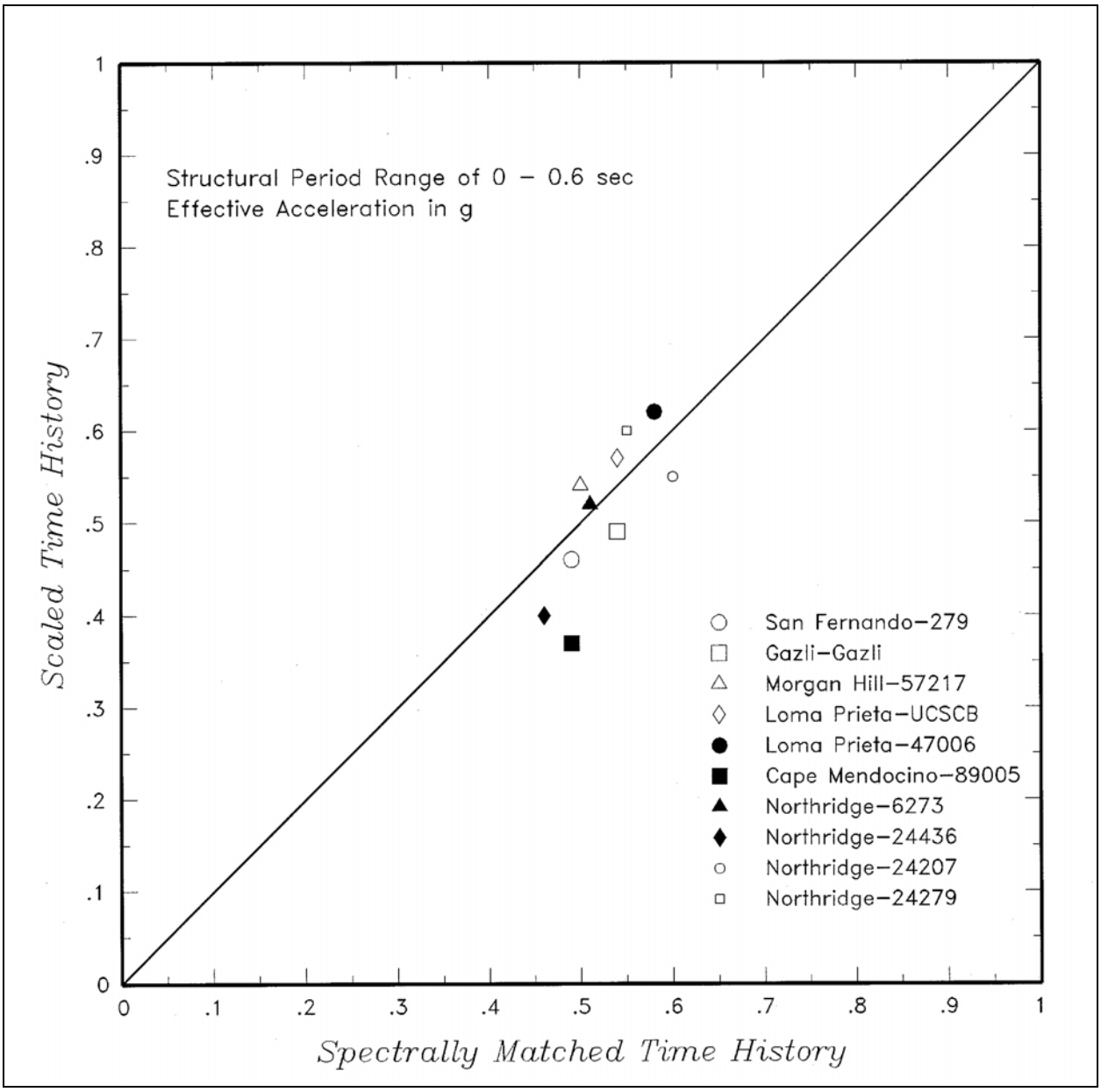

Figure D-33. Comparison for effective peak acceleration estimated from the scaled and spectrally matched time-histories

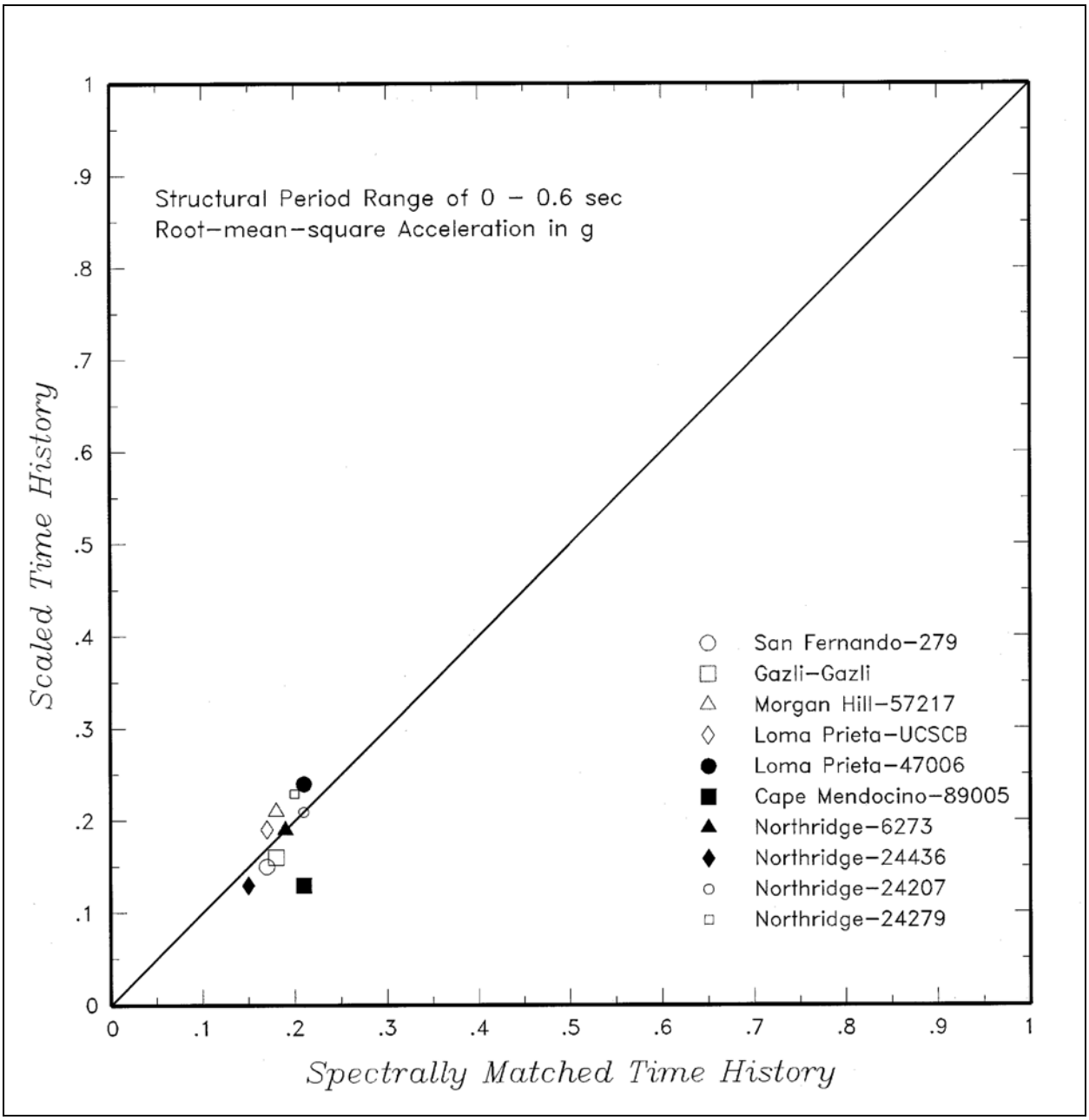

Figure D-34. Comparison for root-mean-square acceleration estimated from the scaled and spectrally matched time-histories

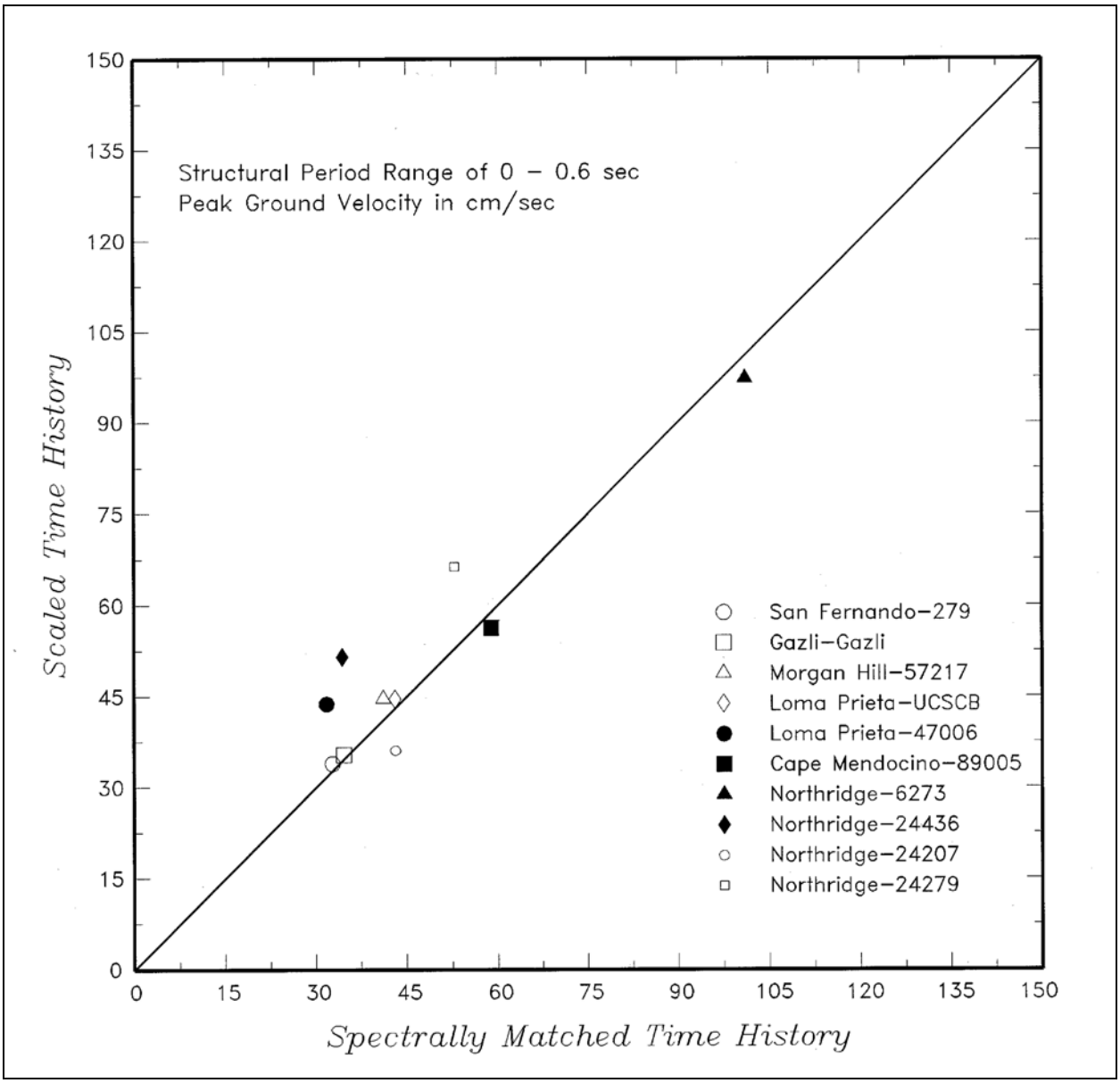

Figure D-35. Comparison for peak velocity estimated for the scaled and spectrally matched time-histories

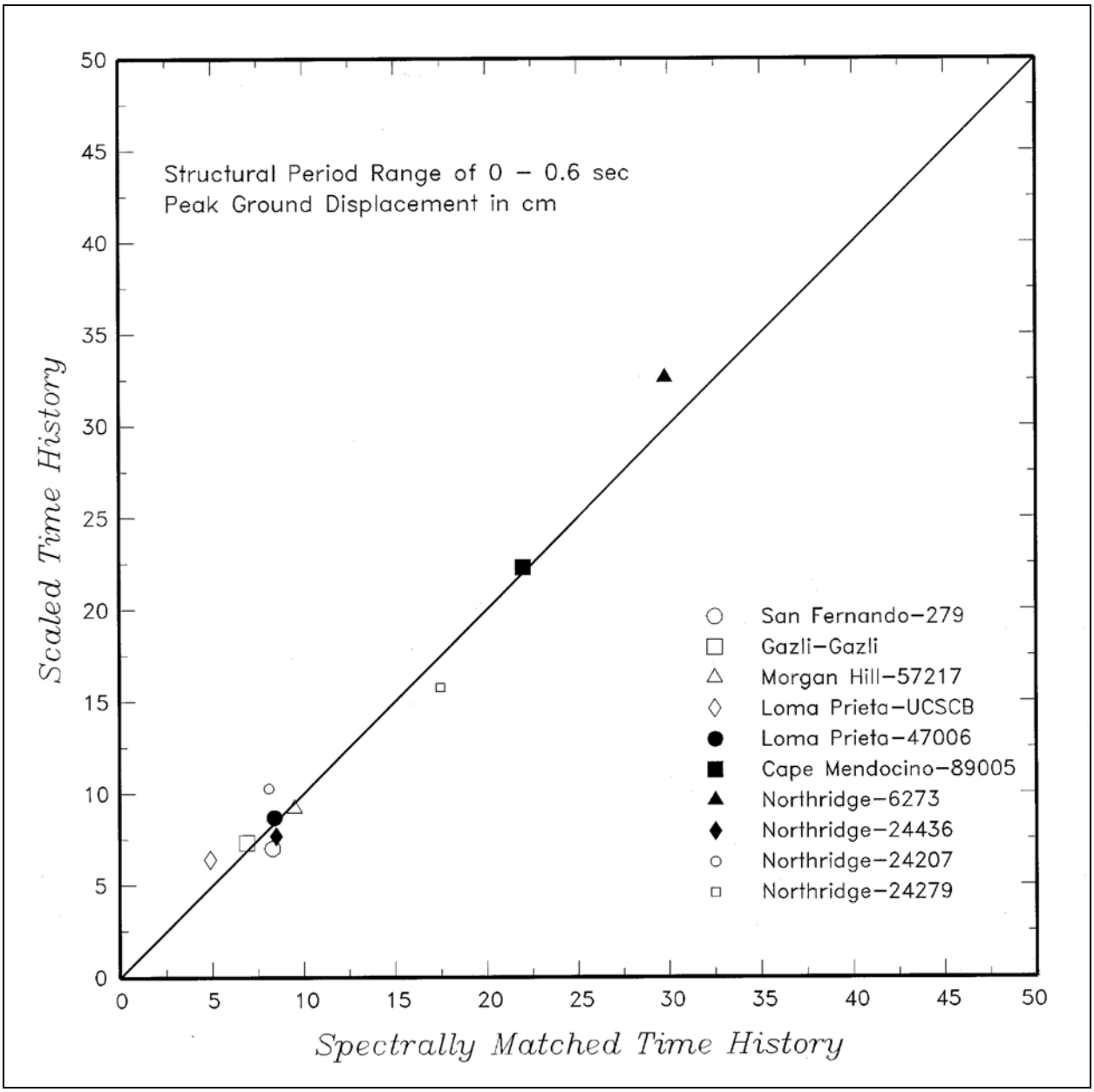

Figure D-36. Comparison for peak displacement estimated for the scaled and spectrally matched time-histories

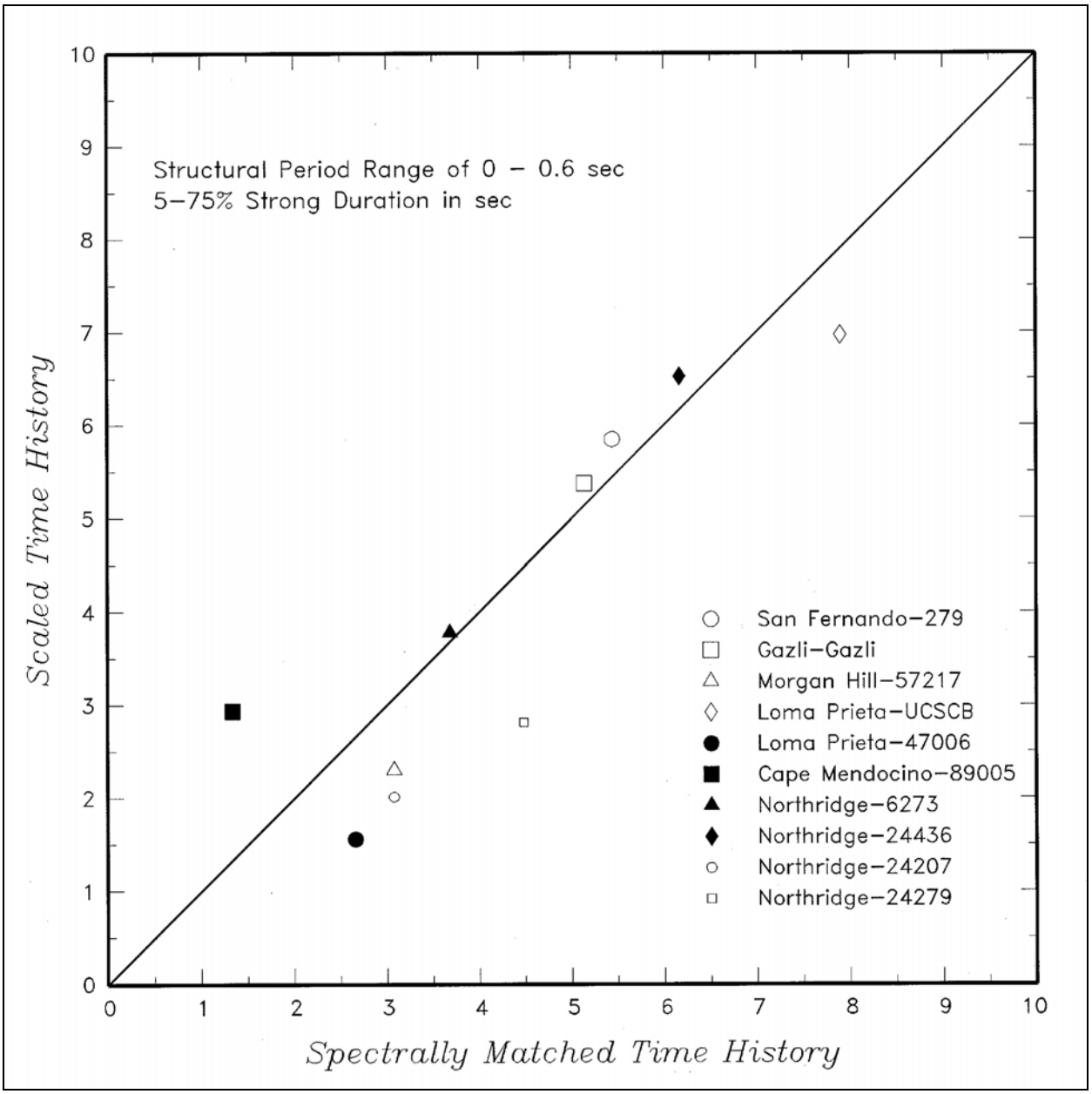

Figure D-37. Comparison for 5 to 75 percent strong duration estimated from the scaled and spectrally matched time-histories

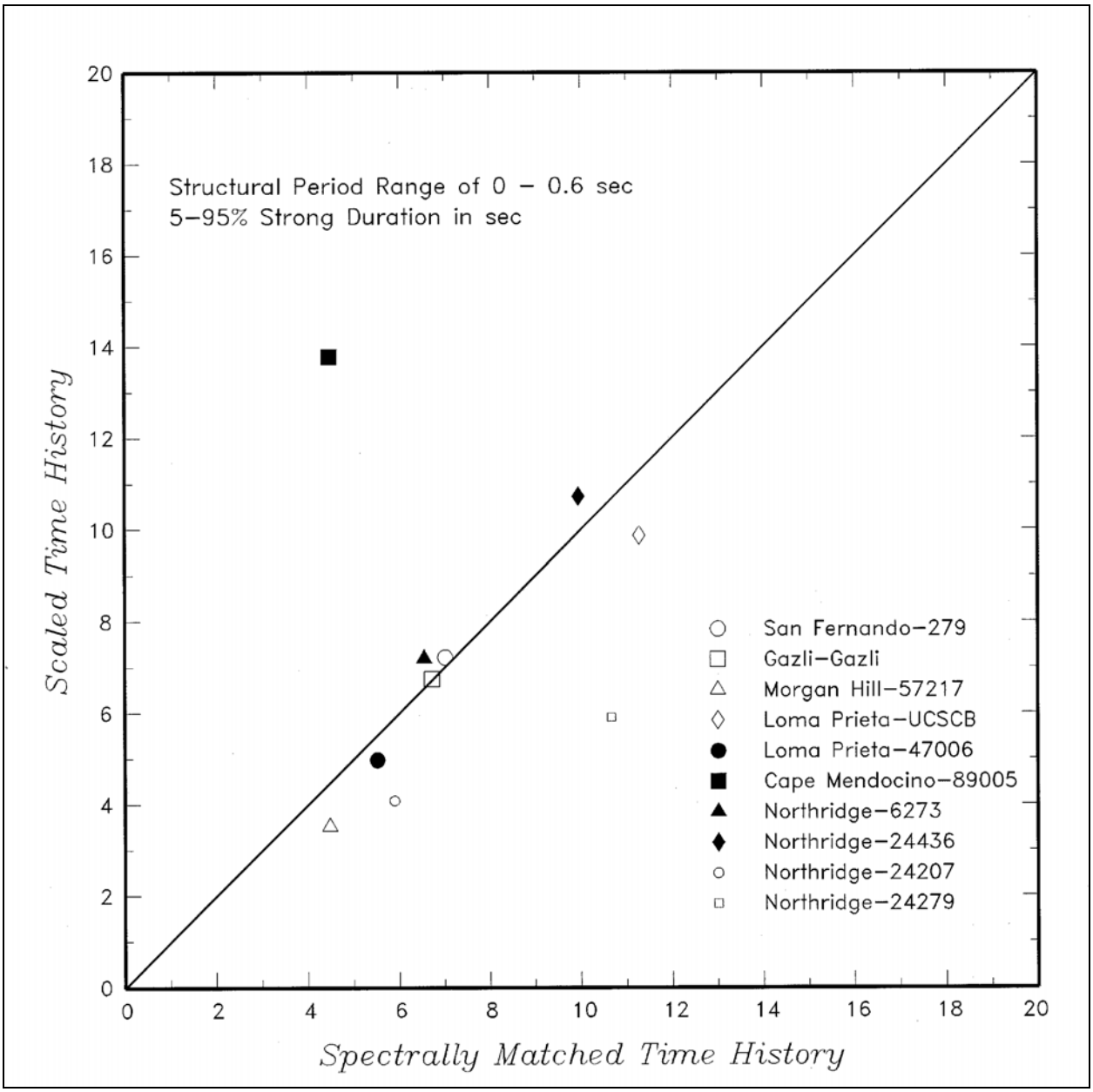

Figure D-38. Comparison for 5 to 95 percent strong duration estimated from the scaled and spectrally matched time-histories

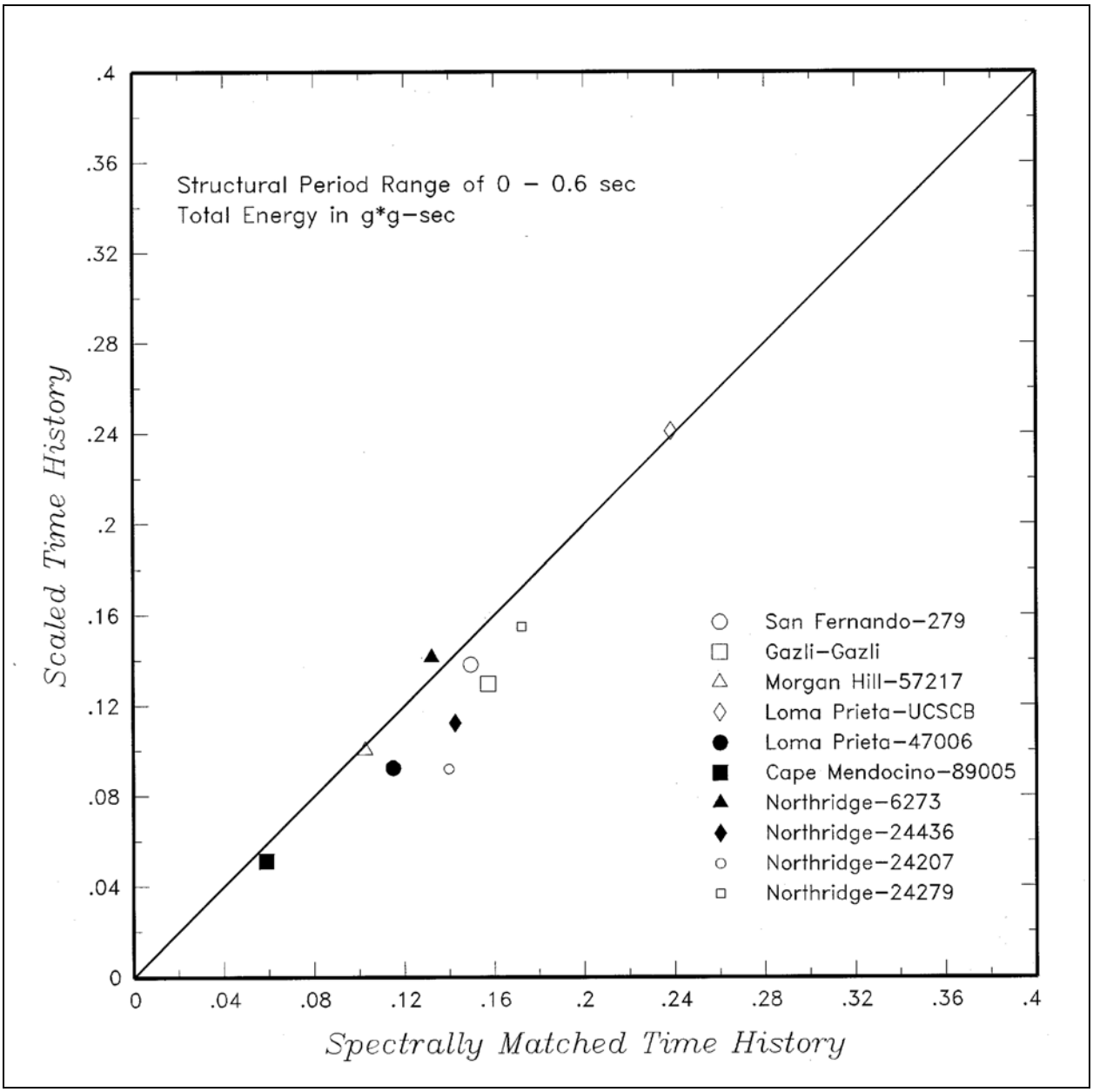

Figure D-39. Comparison for total energy estimated from the scaled and spectrally matched time-histories

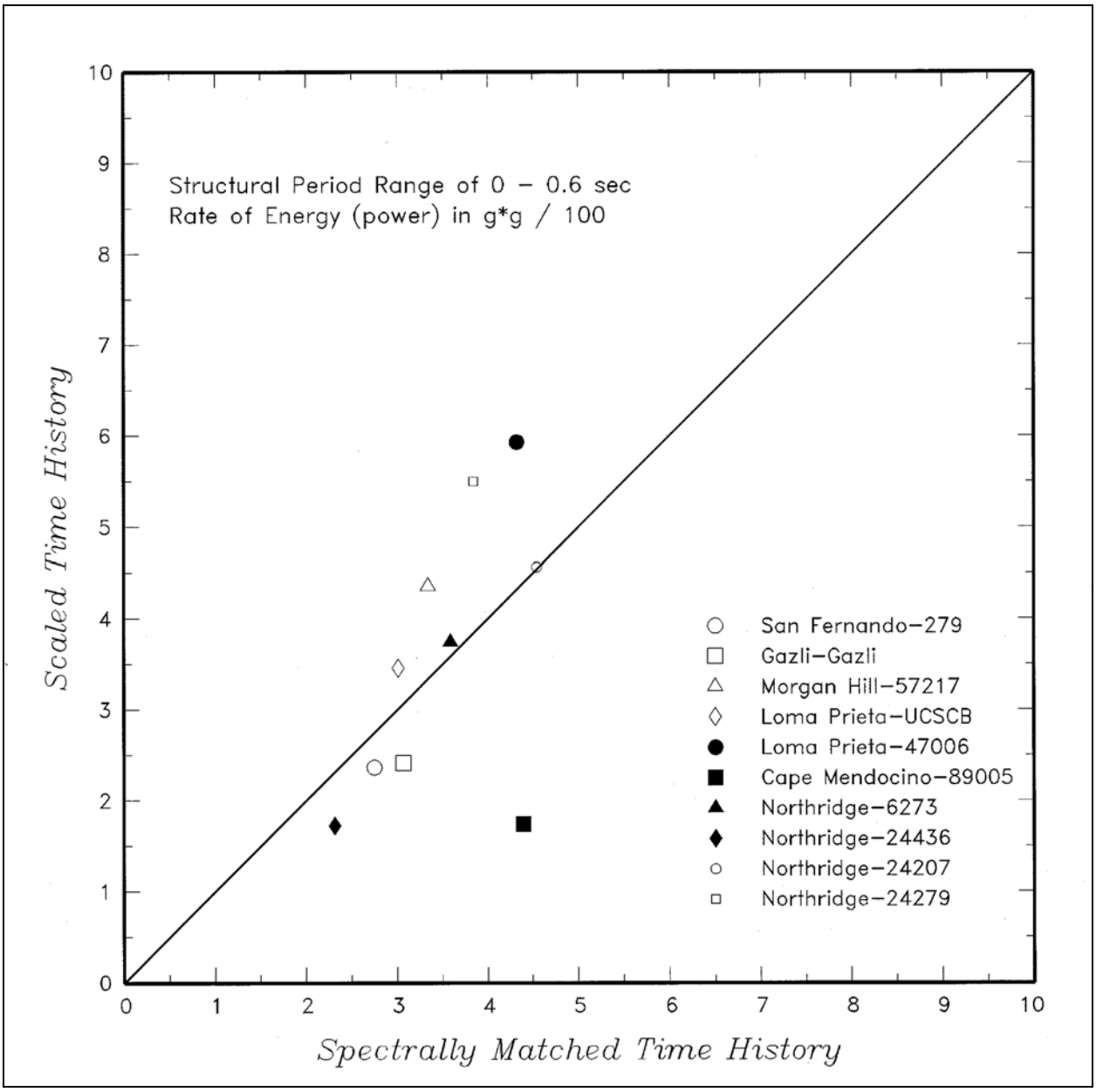

Figure D-40. Comparison for rate of energy (power) estimated from the scaled and spectrally matched time-histories

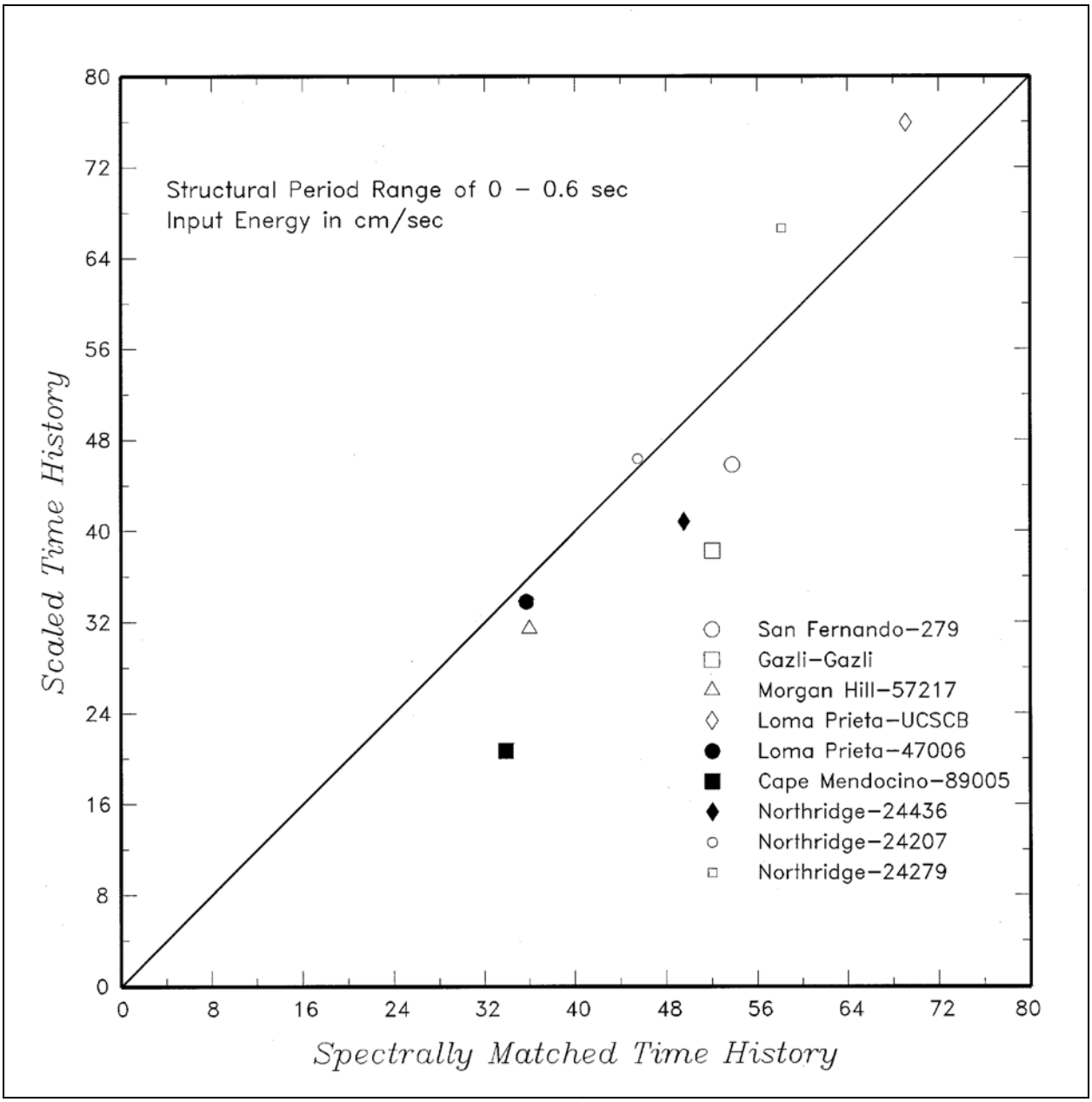

Figure D-41. Comparison for input energy estimated from the scaled and spectrally matched time-histories

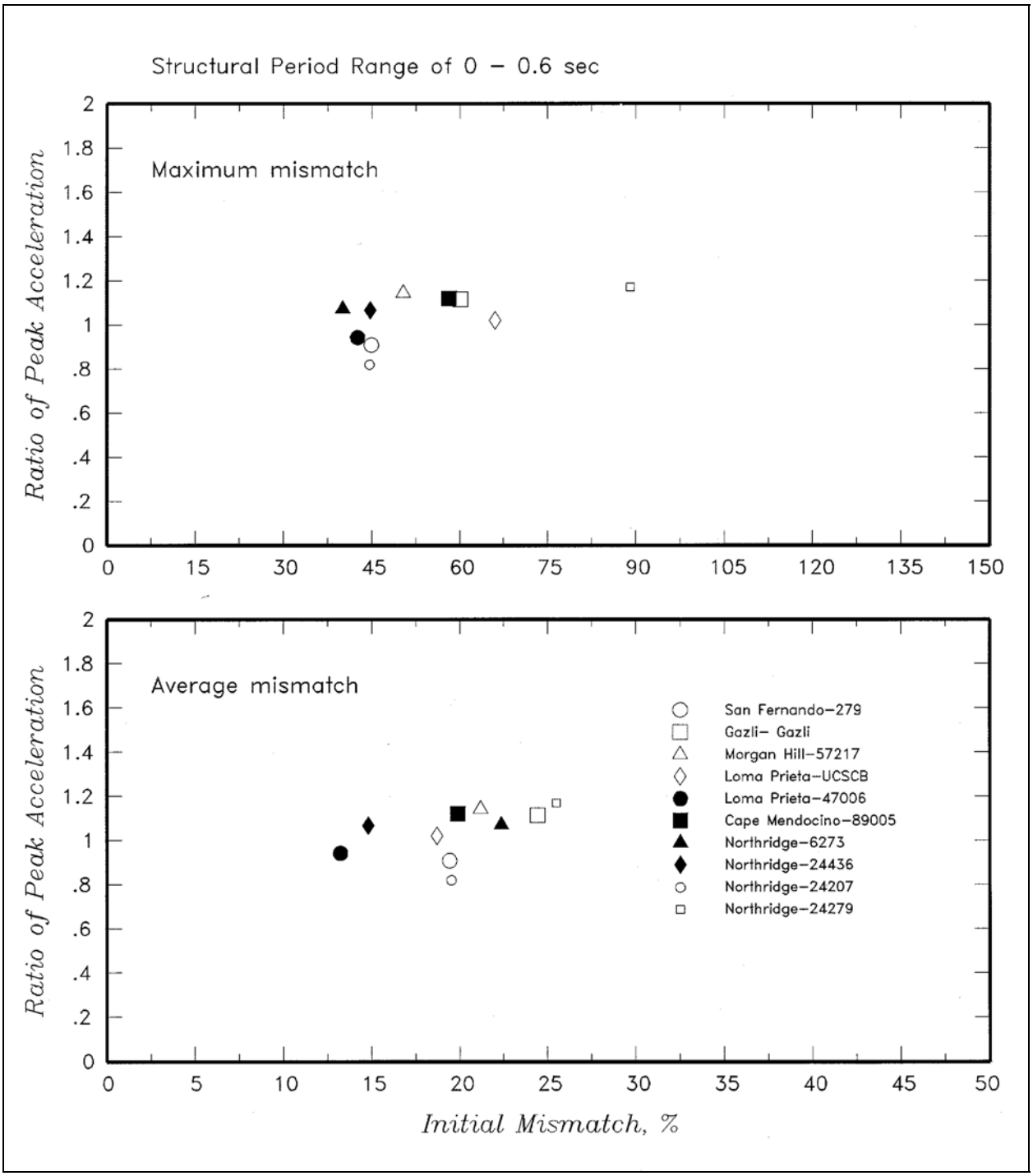

Figure D-42. Relationship between initial mismatch and peak acceleration ratio of spectrally matched and scaled time-histories

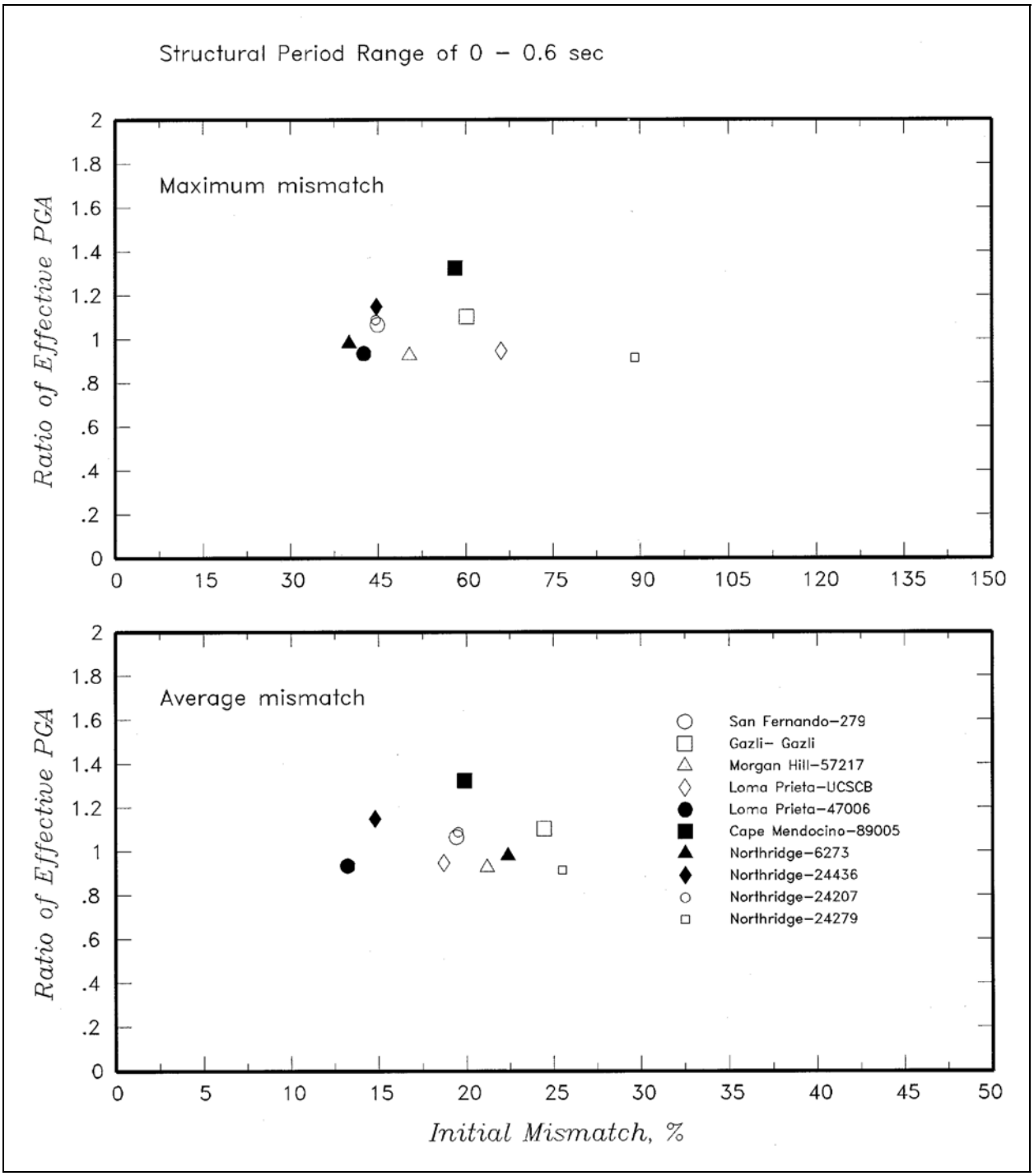

Figure D-43. Relationship between initial mismatch and effective peak acceleration ratio of spectrally matched and scaled time-histories

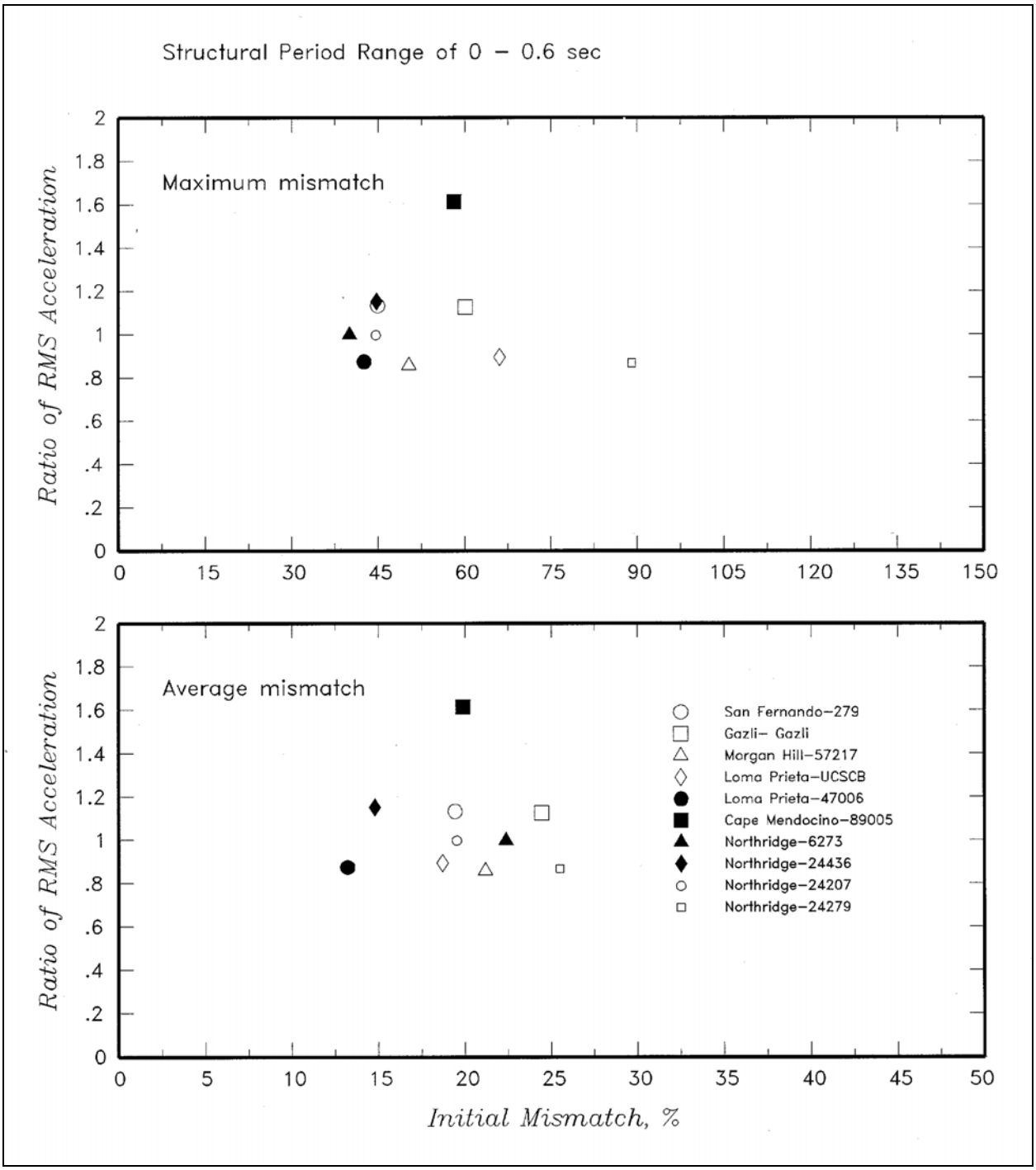

Figure D-44. Relationship between initial mismatch and root-mean-square acceleration ratio of spectrally matched and scaled time-histories

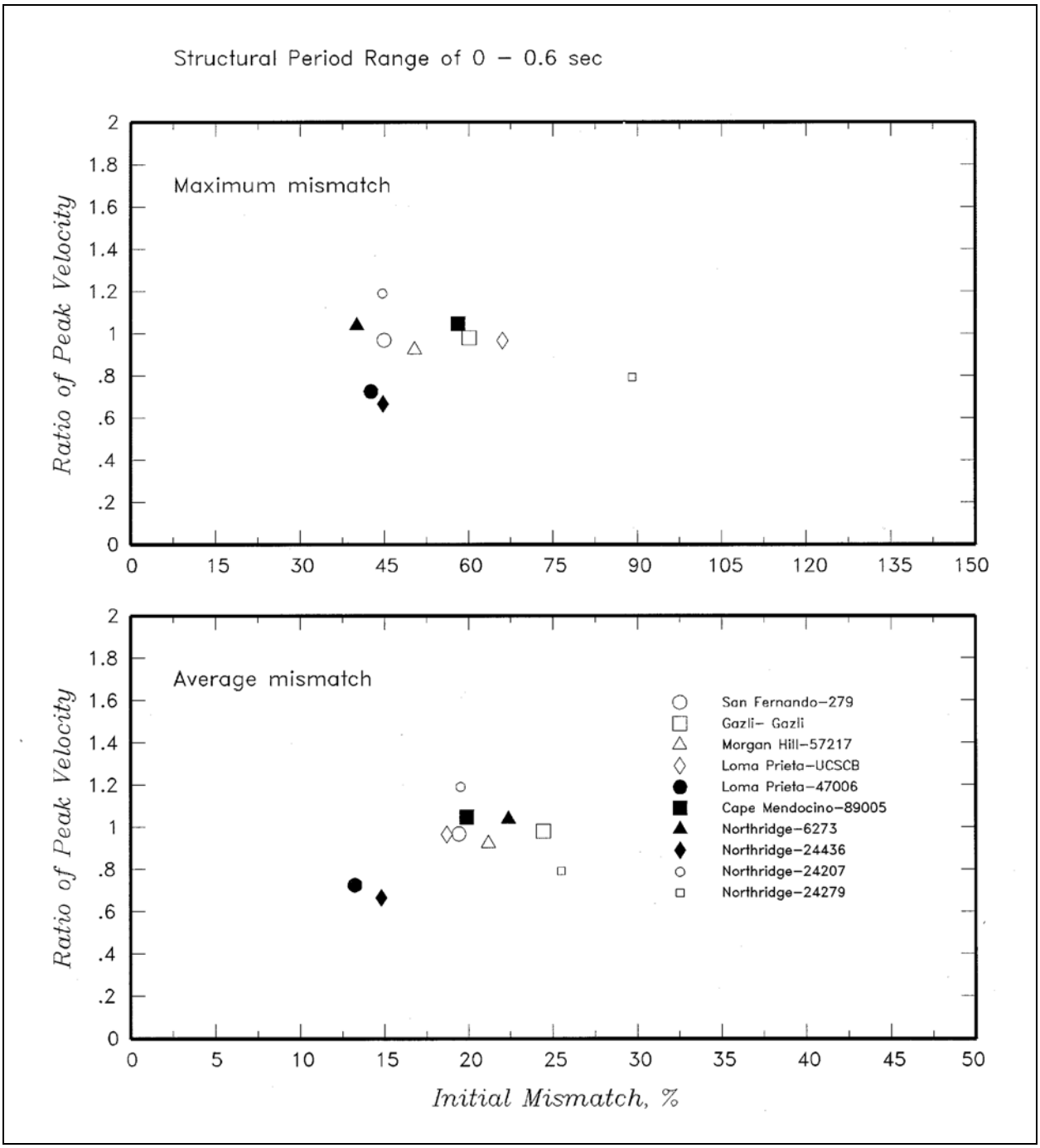

Figure D-45. Relationship between initial mismatch and peak velocity ratio of spectrally matched and scaled time-histories

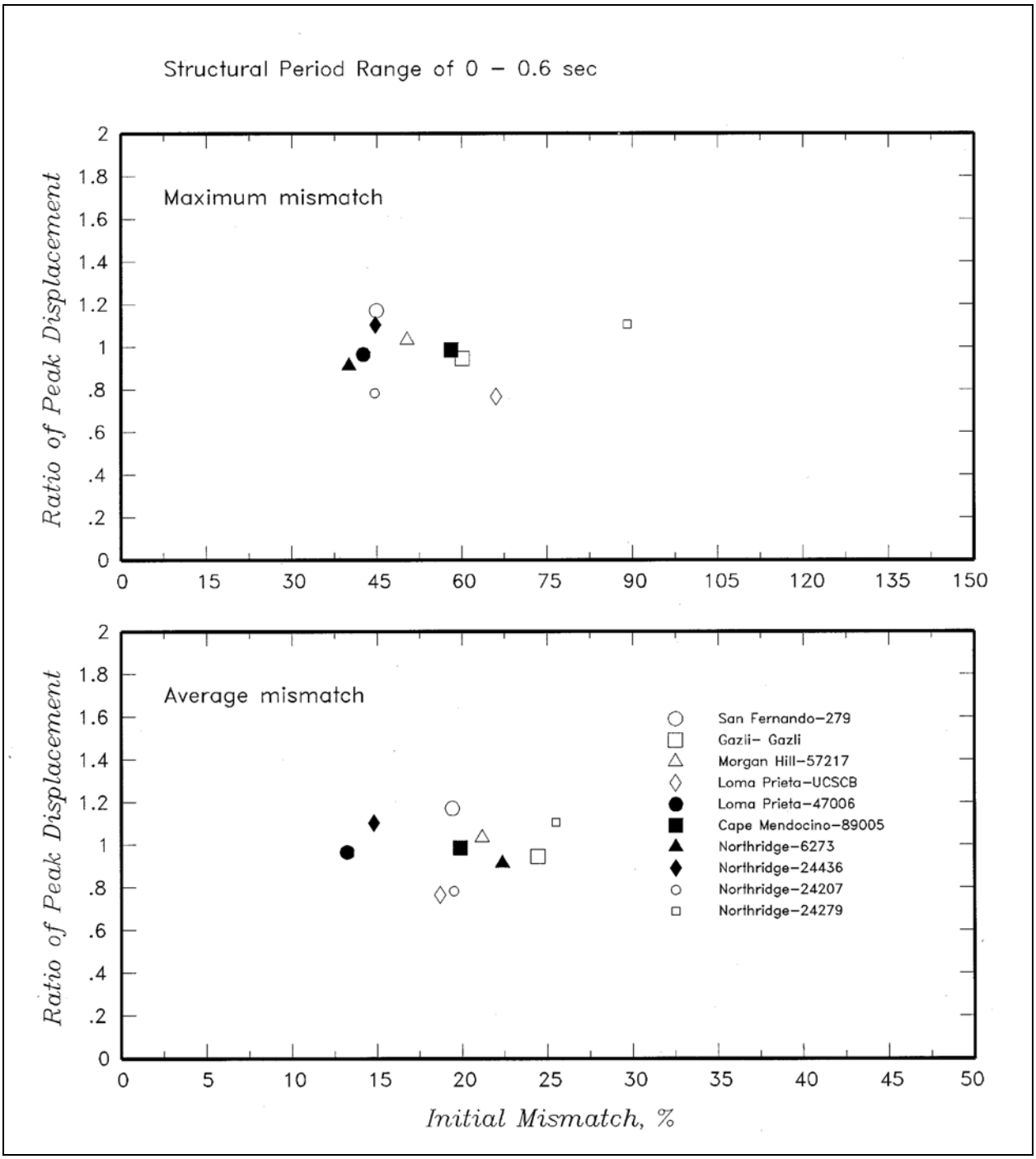

Figure D-46. Relationship between initial mismatch and peak displacment ratio of spectrally matched and scaled time-histories

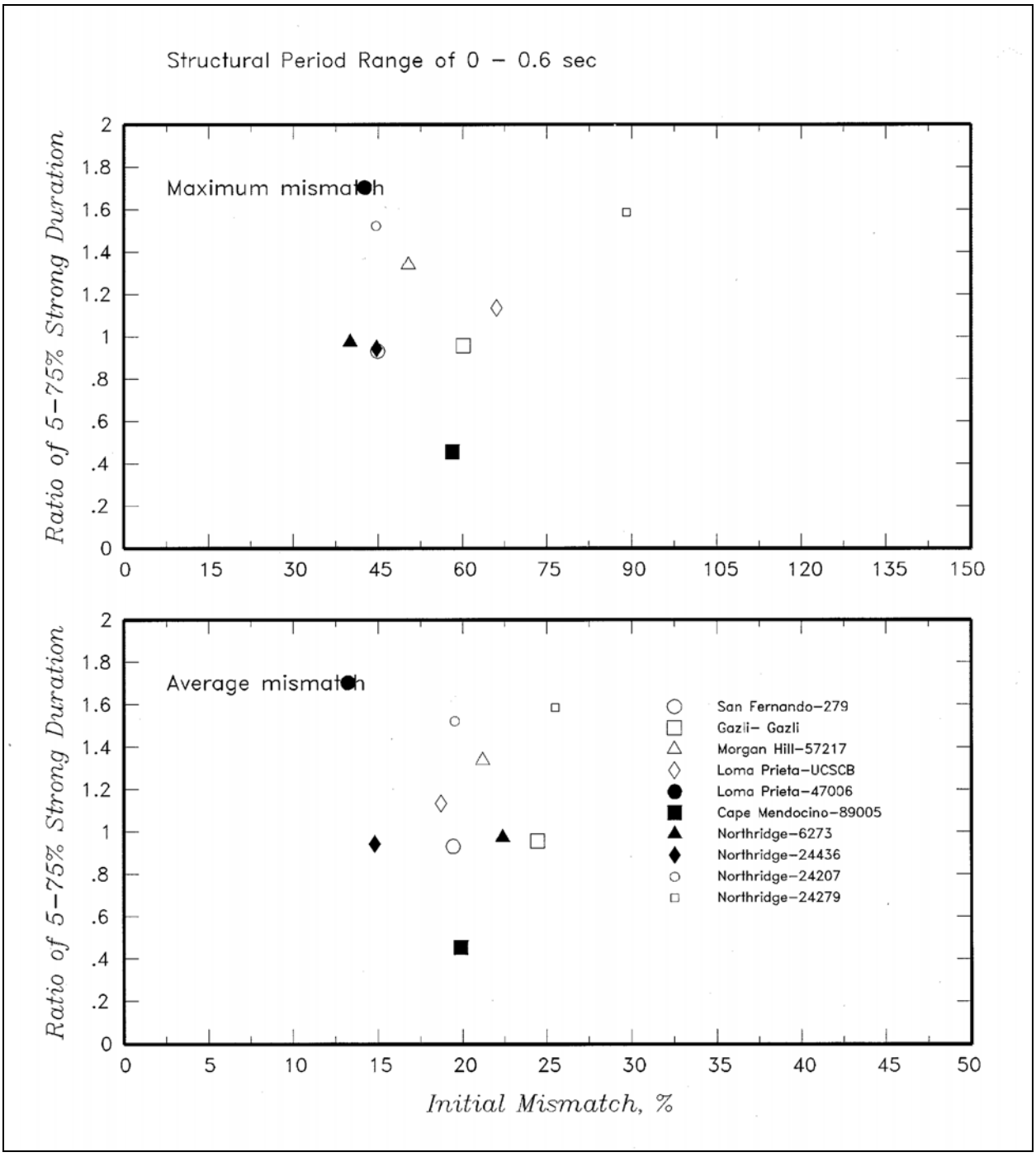

Figure D-47. Relationship between initial mismatch and 5 to 75 percent strong duration ratio of spectrally matched and scaled time-histories

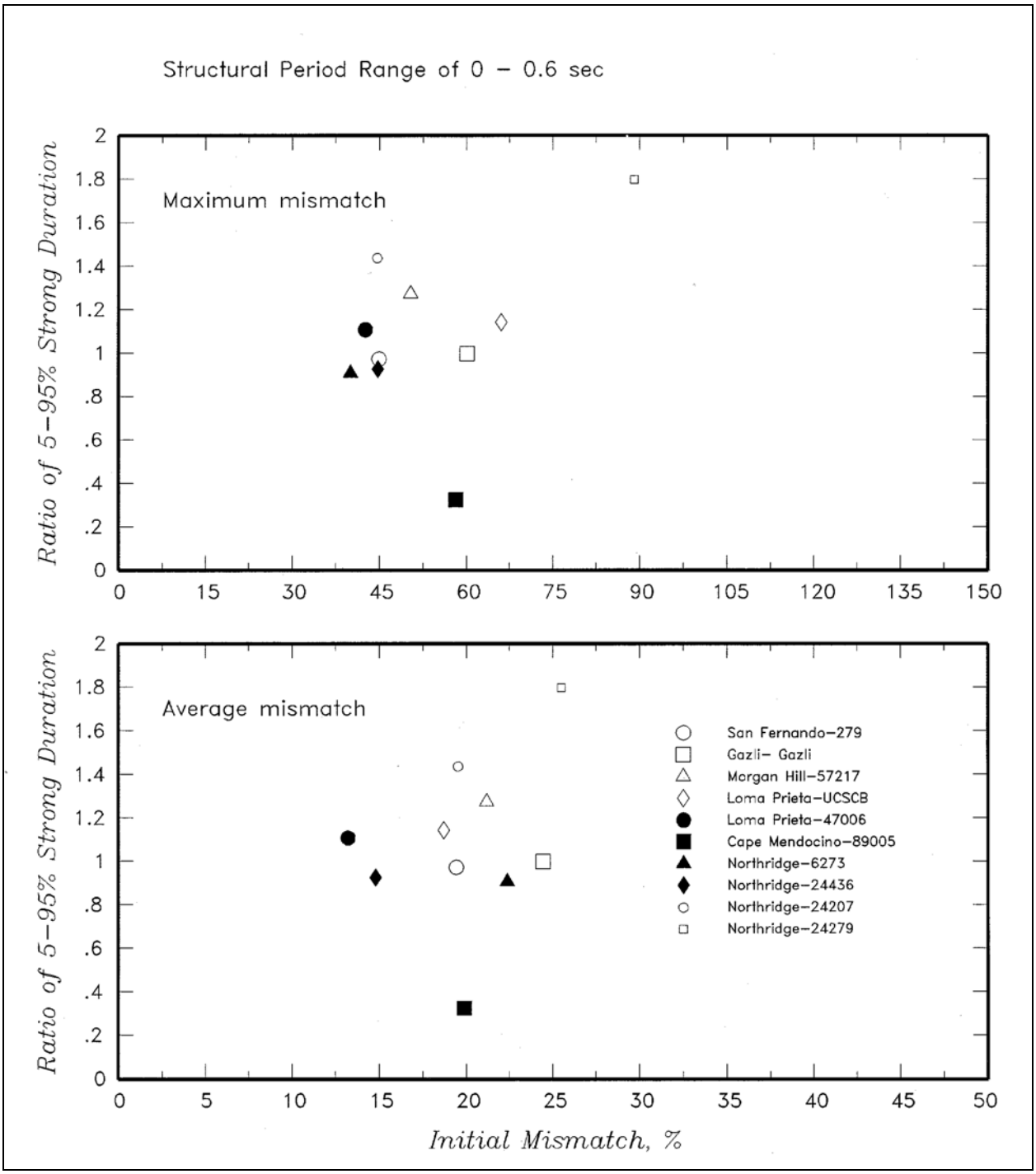

Figure D-48. Relationship between initial mismatch and 5 to 95 percent strong duration ratio of spectrally matched and scaled time-histories

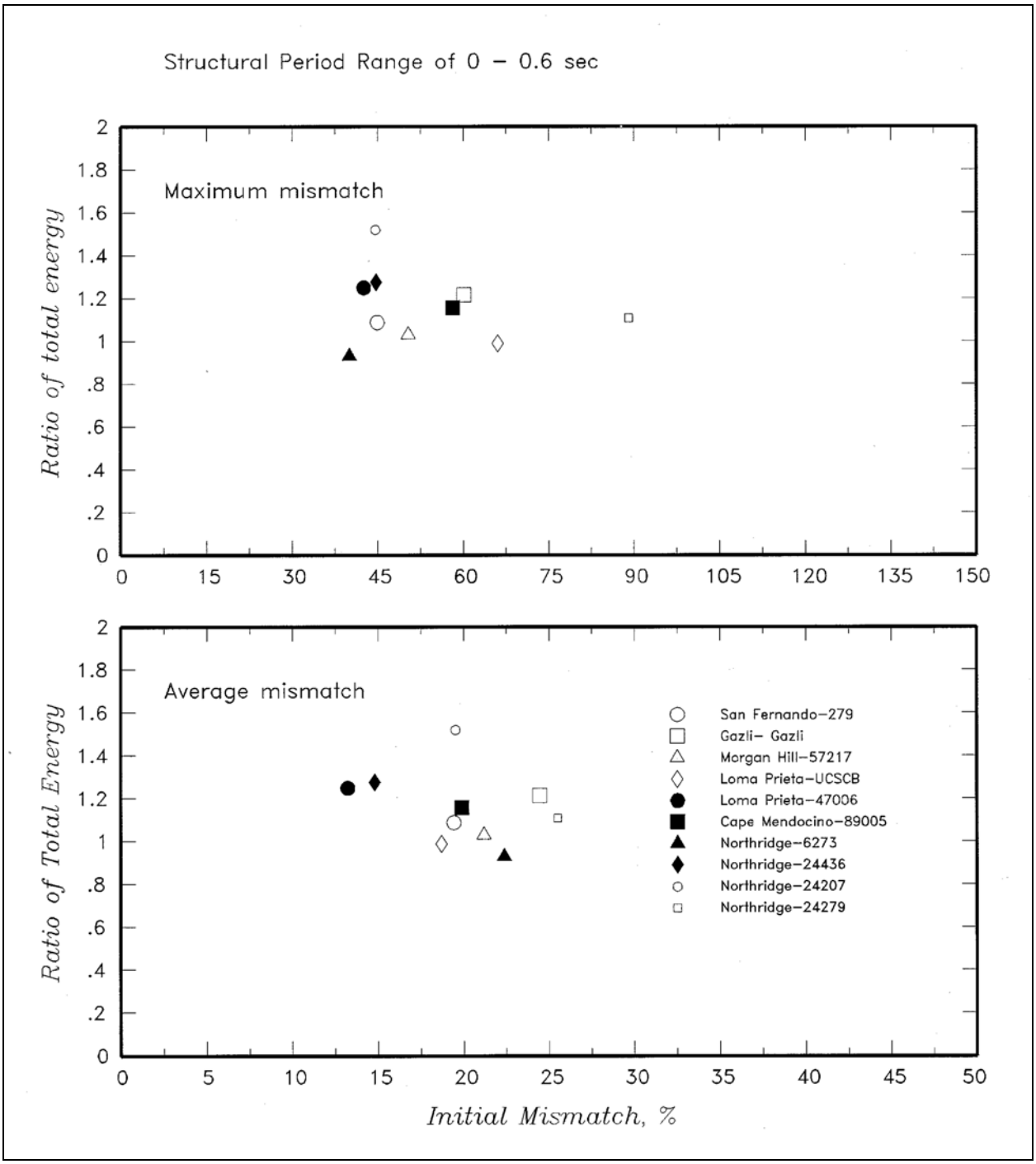

Figure D-49. Relationship between initial mismatch and total energy ratio of spectrally matched and scaled time-histories

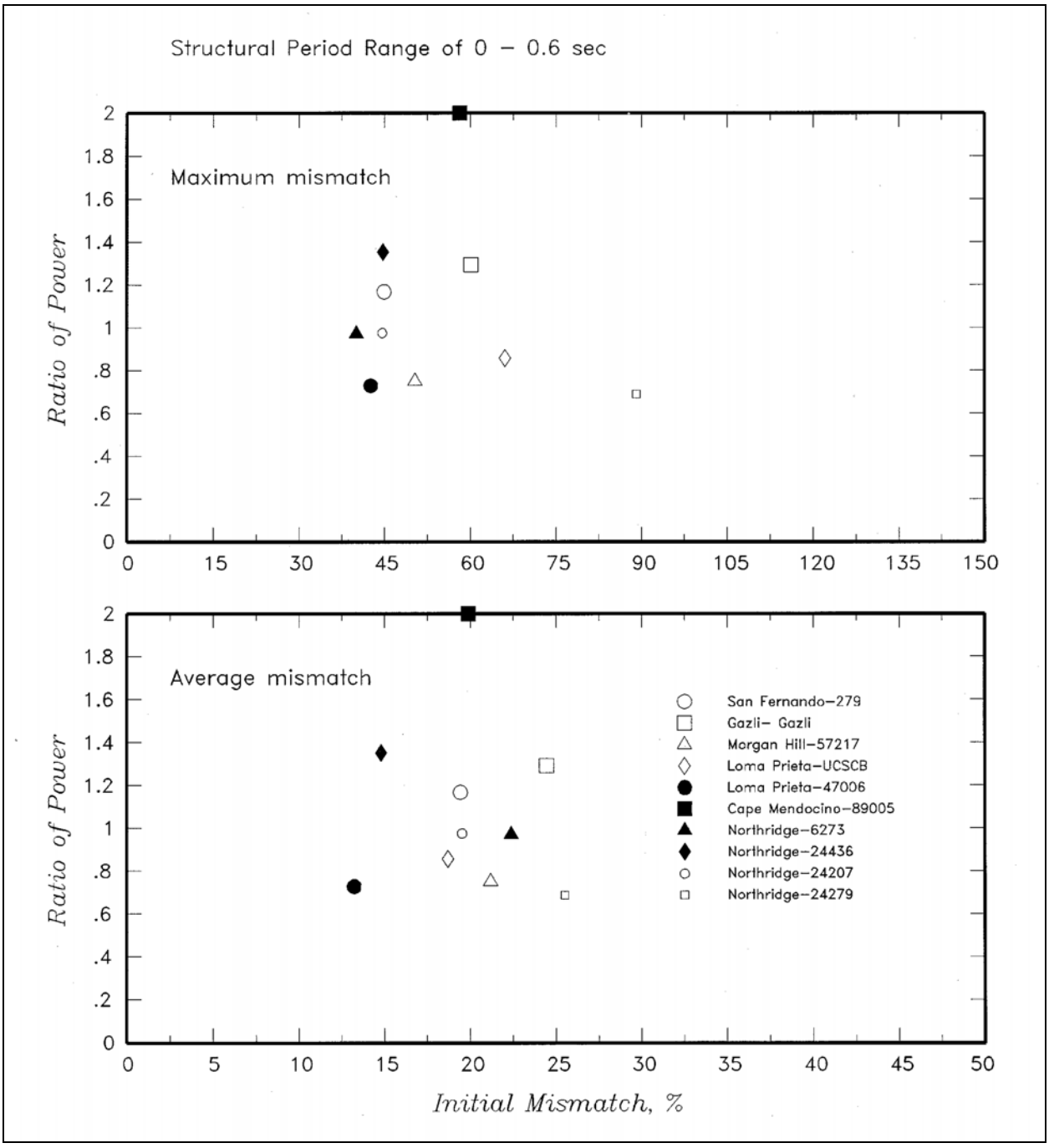

Figure D-50. Relationship between initial mismatch and power ratio of spectrally matched and scaled time-histories

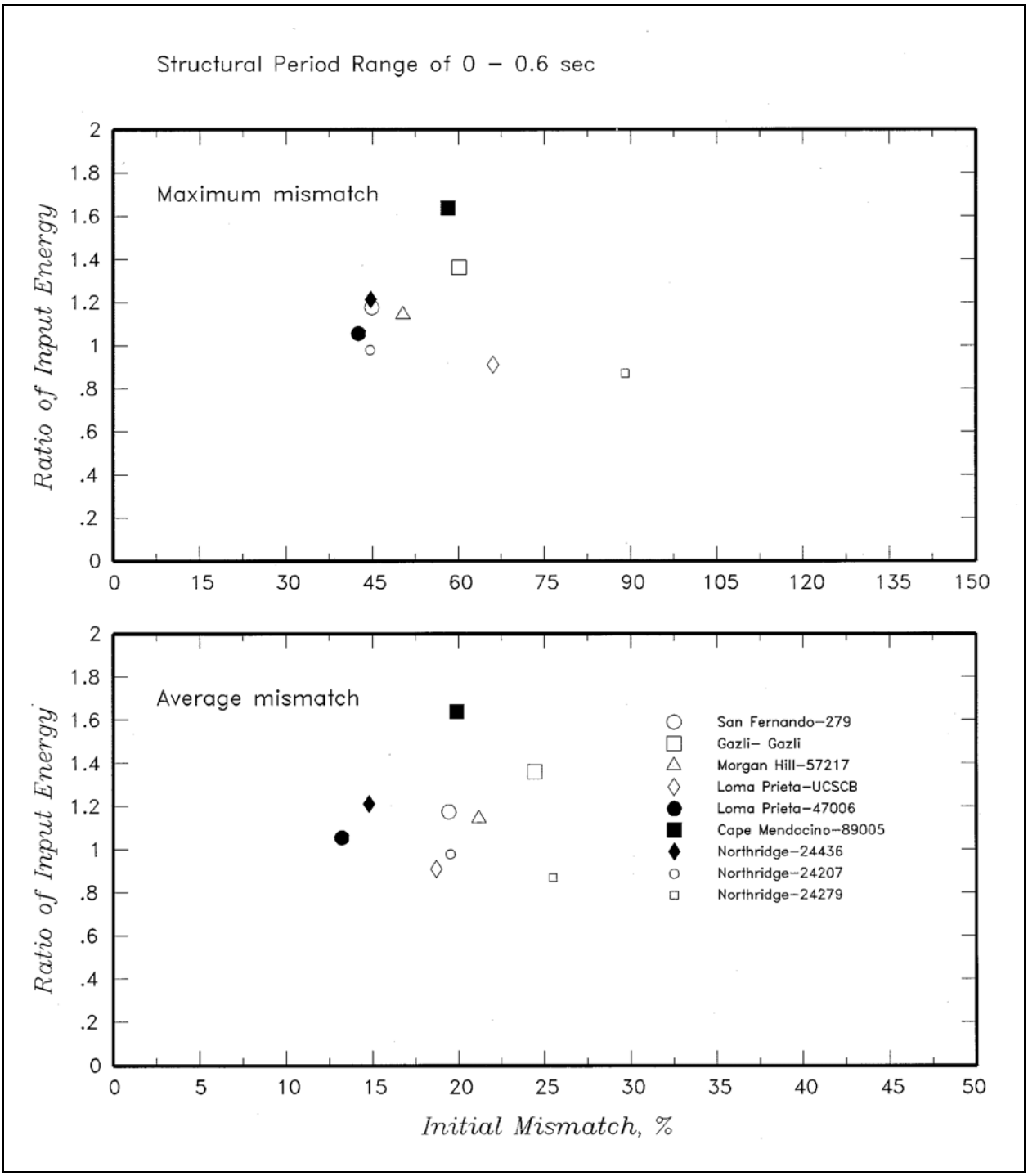

Figure D-51. Relationship between initial mismatch and input energy ratio of spectrally matched and scaled time-histories